

Synergizing Roughness Penalization and Basis Selection in Bayesian Spline Regression

Sunwoo Lim¹ and Seonghyun Jeong^{*1,2}

¹Department of Statistics and Data Science, Yonsei University, Seoul, Korea

²Department of Applied Statistics, Yonsei University, Seoul, Korea

November 23, 2023

Abstract

Bayesian P-splines and basis determination through Bayesian model selection are both commonly employed strategies for nonparametric regression using spline basis expansions within the Bayesian framework. Although both methods are widely employed, they each have particular limitations that may introduce potential estimation bias depending on the nature of the target function. To overcome the limitations associated with each method while capitalizing on their respective strengths, we propose a new prior distribution that integrates the essentials of both approaches. The proposed prior distribution assesses the complexity of the spline model based on a penalty term formed by a convex combination of the penalties from both methods. The proposed method exhibits adaptability to the unknown level of smoothness while achieving the minimax-optimal posterior contraction rate up to a logarithmic factor. We provide an efficient Markov chain Monte Carlo algorithm for implementing the proposed approach. Our extensive simulation study reveals that the proposed method outperforms other competitors in terms of performance metrics or model complexity. An application to a real dataset substantiates the validity of our proposed approach.

Keywords: Nonparametric regression; Bayesian P-splines; Bayesian model selection; posterior contraction rate.

1 Introduction

We consider Bayesian analysis of the nonparametric regression model,

$$y_i = f(x_i) + \epsilon_i, \quad \epsilon_i \stackrel{\text{iid}}{\sim} \text{N}(0, \sigma^2), \quad i = 1, \dots, n, \quad (1)$$

where $f : [0, 1] \rightarrow \mathbb{R}$ is an unknown smooth function, $x_i \in [0, 1]$ are fixed design points, and $\sigma^2 > 0$ is a variance parameter. Although this study focuses on univariate nonparametric regression, the framework readily extends to the multidimensional case. Among various approaches for modeling the nonparametric function f , we employ the classical method that parameterizes f using a series of spline basis functions. Specifically, the function f is assumed to be approximated as a linear

*Corresponding author: sjeong@yonsei.ac.kr

combination of J basis terms, $f(\cdot) = \sum_{j=1}^J \theta_j \psi_j(\cdot)$, where ψ_j is the j th spline basis function and θ_j is the corresponding coefficient. While this classical approach is simple yet effective, it is important to acknowledge that the quality of the resulting estimation heavily depends on the specification of basis functions. Accordingly, it is crucial to carefully control the regularity of the regression function to avoid both underfitting or overfitting, ensuring that the model adapts appropriately to the inherent smoothness of the unknown target function. While there are various approaches to tuning the regularity of spline functions, we will focus on discussing the two widely accepted Bayesian ideas.

The first method, known as Bayesian P-splines, involves fixing a sufficient number of equidistant knots for spline basis functions and regularizing the function by penalizing adjacent spline coefficients (Lang and Brezger, 2004). The approach inherits advantages from the classical penalized splines, including computational simplicity of the penalty and moment conservation of the data (Eilers and Marx, 1996). Moreover, it offers additional benefits compared to the frequentist counterpart, providing coverage probability estimation and efficient smoothing parameter estimation in additive models with numerous function components (Lang and Brezger, 2004; Wood, 2006, 2011). However, despite their notable advantages, Bayesian P-splines have a few drawbacks. One major limitation is that the prior variance of the nonparametric function is highly dependent on the user-specified number of knots (Ventrucci and Rue, 2016). Moreover, empirical evidence suggests that Bayesian P-splines often suffer from overfitting issues due to the prior on the roughness penalty (Simpson et al., 2017). It has also been reported that using an excessive number of knots can lead to increased mean squared errors (MSEs) in penalized splines (Ruppert, 2002). Considering these points collectively, it becomes evident that determining an appropriate number of knots is crucial to optimize the performance of Bayesian P-splines. Another limitation of Bayesian P-splines is a lack of comprehensive understanding of its theoretical properties. Recently, Bach and Klein (2021) established the posterior contraction rates for Bayesian P-splines. However, their rates are not adaptive, and achieving the optimal rate requires knowing the smoothness parameter in advance.

The second approach builds upon Bayesian model selection (BMS) to determine the best configuration of the basis functions (Denison et al., 1998; DiMatteo et al., 2001; Liang et al., 2008; Smith and Kohn, 1996). In this method, the smoothness of the function is directly characterized by the knot locations, without imposing further regularization on the spline coefficients. The number of knots, and occasionally their specific locations to enhance flexibility, are determined based on the posterior probability of the basis models. We refer to this approach as Bayesian basis selection. The major advantage of using Bayesian basis selection is its adaptivity in achieving the optimal posterior contraction rates even when the smoothness parameter of the target function is unknown (Belitser and Serra, 2014; De Jonge and Van Zanten, 2012; Shen and Ghosal, 2015). It is essential to employ a suitable prior distribution for Bayesian model selection (Kass and Raftery, 1995; Liang et al., 2008). Conventionally, Zellner’s g-prior (Zellner, 1986) and its mixture priors (Liang et al., 2008; Li and Clyde, 2018; Kang and Jeong, 2023) are commonly used. The g-prior (or its mixture form) is preferred for its efficient computation and invariance to transformations (Liang et al., 2008). Conceptually, it bears a connection to classical information theory-based criteria, such as the Akaike information criteria (AIC) and the Bayesian information criteria (BIC) (George and Foster, 2000). However, in the context of Bayesian basis selection for nonparametric

regression, the g-prior and mixture priors penalize complex models based on the magnitude of deviations from the center, rather than quantifying its smoothness through measures like the second derivative of f . Hence, while they are effective in selecting a parsimonious model size through Bayesian model selection, they do not offer additional smoothness regularization. This limitation should not be overlooked, as comparing different numbers of basis terms involves evaluating only a few discrete models among infinitely many possibilities, making the resulting function estimation highly sensitive to the chosen knot locations due to model misspecification. This sensitivity often leads to underfitting, favoring a smaller model over a larger one when unable to choose the best model that lies between the two. In this context, incorporating additional smoothness regularization can prove to be advantageous even after selecting an appropriate number of basis functions.

In this study, we propose a new approach that synergizes the strengths of both Bayesian P-splines and Bayesian basis selection, effectively addressing the limitations of each method by introducing a new prior distribution. Our suggested prior involves penalizing both the sizes of f and the second derivative of f , offering effective regularization for both basis selection and smoothness control of the regression function. The proposed prior is viewed as a fusion of the penalty priors for the Bayesian P-spline prior and the g-prior for Bayesian basis selection, comprising a convex combination of two penalty matrices. By integrating these complementary aspects into the prior, our method provides a comprehensive and robust framework that can adaptively determine the number of basis functions while simultaneously ensuring the desired level of smoothness in the estimated function. The proposed method has been demonstrated to outperform other competitors or yield a more parsimonious model complexity than methods with comparable performance. Figure 1 substantiates the empirical performance of the proposed method across a few specified functions. Meanwhile from a theoretical standpoint, we show that the proposed method can adapt to unknown smoothness levels, achieving the optimal posterior contraction rates, which is a remarkable feature not yet achieved by the conventional Bayesian P-spline approach (Bach and Klein, 2021).

The remainder of the paper is organized as follows. In Section 2, we provide an overview of Bayesian P-splines and Bayesian basis selection. Section 3 describes the proposed method that integrates both approaches, accompanied by a well-specified prior distribution and a Markov chain Monte Carlo (MCMC) algorithm. Theoretical analysis for the proposed method, establishing the posterior contraction rate, is provided in Section 4. Section 5 presents an extensive simulation study, while an application of the proposed method to a real dataset is discussed in Section 6. Technical proofs and additional details on the sampling algorithm are presented in Appendix.

2 Preliminaries

In this section, we offer an overview of Bayesian P-splines and Bayesian basis selection. These methods serve as the foundational components that constitute our proposed method in Section 3.

To begin, we first establish the mathematical notation. For sequences a_n and b_n , we write $a_n \lesssim b_n$ (or $b_n \lesssim a_n$) to imply that $a_n \leq cb_n$ for a universal constant c independent of n . The notation $a_n \asymp b_n$ implies $a_n \lesssim b_n$ and $a_n \gtrsim b_n$. For a continuous function $g : [0, 1] \rightarrow \mathbb{R}$, $\|g\|_\infty = \sup_{x \in [0, 1]} |g(x)|$ denotes the supremum norm, $\|g\|_2 = (\int |g(x)|^2 dx)^{1/2}$ denotes the L_2 -

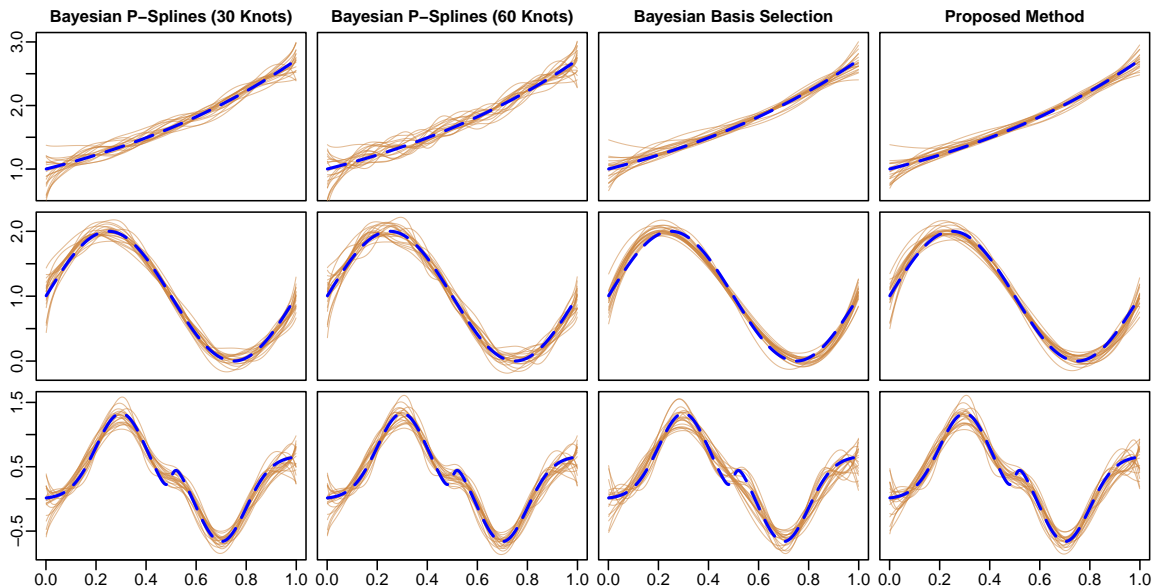


Figure 1: Pointwise posterior means (gold solid) of 20 replicated datasets generated with the true functions (blue dashed) using $n = 200$ and $\sigma = 0.5$. The estimation results show that Bayesian P-splines are sensitive to the number of prespecified knots and frequently display overfitting. On the other hand, Bayesian basis selection (with the Zellner-Siow prior; see Section 2.2) exhibits significant estimation bias due to model misspecification. The proposed method strikes a balance between the advantages of the two methods.

norm, and $\|g\|_n = (n^{-1} \sum_{i=1}^n |g(x_i)|^2)^{1/2}$ denotes the empirical L_2 -norm. We use the notation Π to represent the prior or posterior measure, while π is used to denote the corresponding density with respect to the dominating measure.

2.1 Bayesian P-Splines

Bayesian P-splines are a widely utilized tool for function estimation (Lang and Brezger, 2004), offering a Bayesian counterpart to the penalized splines (Eilers and Marx, 1996). In this approach, the nonparametric function f is represented through a specific set of basis functions known as B-splines (De Boor, 1978). Specifically, Bayesian P-splines are characterized by the B-spline basis terms determined by a collection of equally spaced interior knots, denoted as $0 = \xi_0 < \xi_1 < \dots < \xi_K < \xi_{K+1} = 1$. As a result, for a polynomial degree l , we generate $J = l + K + 1$ terms of B-spline basis functions. The value J for the basis terms is fixed to a suitably large number capable of capturing the local and global signals of the target function.

Let $x \mapsto \{B_1(x), B_2(x), \dots, B_J(x)\}$ be the B-spline basis functions such that f is expressed as $f(\cdot) = \sum_{j=1}^J \theta_j B_j(\cdot)$. Let $\mathbf{B}_J \in \mathbb{R}^{n \times J}$ represent the basis matrix with $B_j(x_i)$ for the (i, j) th element. (Although J is fixed in advance for Bayesian P-splines, we introduce the subscript here and in what follows to maintain notational consistency with the subsequent sections.) Bayesian P-splines are characterized by putting an improper prior on the corresponding spline coefficients

$\boldsymbol{\theta}_J = (\theta_1, \dots, \theta_J)^T \in \mathbb{R}^J$, that is,

$$\pi(\boldsymbol{\theta}_J \mid \lambda) \propto \frac{1}{\lambda^{\text{rank}(\mathbf{P}_J)/2}} \exp\left(-\frac{1}{2\lambda} \boldsymbol{\theta}_J^T \mathbf{P}_J \boldsymbol{\theta}_J\right), \quad (2)$$

where $\mathbf{P}_J = \mathbf{D}_J^T \mathbf{D}_J$ is the penalty matrix with \mathbf{D}_J a matrix representing a finite difference operation that renders smoothness of the function. Throughout the paper, we use the second-order finite difference matrix defined as

$$\mathbf{D}_J = \begin{pmatrix} 1 & -2 & 1 & 0 & \dots & 0 & 0 & 0 & 0 \\ 0 & 1 & -2 & 1 & \dots & 0 & 0 & 0 & 0 \\ \vdots & \vdots & \vdots & \vdots & \ddots & \vdots & \vdots & \vdots & \vdots \\ 0 & 0 & 0 & 0 & \dots & 0 & 1 & -2 & 1 \end{pmatrix} \in \mathbb{R}^{(J-2) \times J}.$$

Since the prior in (2) is not invariant to scaling of the response variable, it is commonly advised to standardize the response vector \mathbf{y} (Lang and Brezger, 2004).

When considering B-splines with equidistant knots, it is well known that the term $\boldsymbol{\theta}_J^T \mathbf{P}_J \boldsymbol{\theta}_J$ serves as an approximation for an L_2 -penalty on the squared second derivative, that is, $\|f''\|_2^2 = \int (f''(x))^2 dx$ (Eilers and Marx, 1996; Xiao, 2019). The resulting conditional posterior can be interpreted as

$$-\log \pi(f \mid \mathbf{y}, \lambda, \sigma^2) \approx -\log\text{-likelihood} + \frac{1}{2\lambda} \|f''\|_2^2 + c, \quad (3)$$

for some constant c independent of the coefficients. As a consequence, Bayesian P-splines are considered a procedure that directly imposes a penalty on the smoothness of the target function through the prior distribution.

The dispersion parameter λ plays a crucial role in determining the level of smoothness, similar to the smoothing parameter in frequentist penalized splines. It is commonly assigned an inverse gamma prior, $\lambda \sim \text{IG}(a_\lambda, b_\lambda)$, with $a_\lambda > 0$ and $b_\lambda > 0$. To take advantage of semi-conjugacy, the variance parameter σ^2 is also assigned an inverse gamma prior, $\sigma^2 \sim \text{IG}(a_\sigma, b_\sigma)$, with $a_\sigma \geq 0$ and $b_\sigma \geq 0$. (We include zero hyperparameters to informally represent the Jeffreys prior as a member of the inverse gamma family.) It is well known that the posterior resulting from (2) is proper under very mild conditions as long as the prior on λ is proper with $a_\lambda > 0$ and $b_\lambda > 0$, even when the Jeffreys prior is used for σ^2 (i.e., $a_\sigma = 0$ and $b_\sigma = 0$) (Fahrmeir and Kneib, 2009).

Bayesian P-splines have achieved widespread success and have found applications in numerous function estimation problems (Baladandayuthapani et al., 2005; Hennerfeind et al., 2006; Brezger and Lang, 2006). One of the key factors contributing to its success is its efficient and straightforward implementation. However, despite its apparent advantages, there are a few notable drawbacks associated with Bayesian P-splines. First, the prior variance of the nonparametric function is highly reliant on the number of knots specified by the user in advance (Ventrucci and Rue, 2016), thereby making the estimation results sensitive to the chosen number of knots. As a result, it is beneficial to carefully select the appropriate number of knots to ensure the effective use of Bayesian P-splines (Ruppert, 2002). Moreover, the use of an inverse gamma prior on λ can lead to overfitting in function estimation, as it lacks sufficient mass around very small λ values (Simpson et al., 2017). These shortcomings are also evident in Figure 1. Thus, it is desirable to

avoid overfitting by refraining from employing an excessive number of knots. Another downside is that the theoretical properties of Bayesian P-splines are not as well understood compared to the basis selection approaches. Although [Bach and Klein \(2021\)](#) recently examined the posterior contraction rates for Bayesian P-splines, these rates are not adaptive, and achieving the optimal rate requires knowing the smoothness parameter in advance. In contrast, Bayesian basis selection enjoys adaptive inference capabilities ([Shen and Ghosal, 2015](#); [Belitser and Serra, 2014](#)).

2.2 Bayesian Basis Selection

Another strategy of regularization in Bayesian spline regression is Bayesian basis selection. This method seeks to identify the optimal knot specification in a data-driven manner, based on BMS. Conventionally, Bayesian basis selection aligns with the principles of Bayesian model averaging ([Hoeting et al., 1999](#)), as it averages across various knot specifications using the posterior distribution, as opposed to selecting a single configuration with the highest posterior probability ([Smith and Kohn, 1996](#); [Kohn et al., 2001](#)). To determine the optimal knot specification, one can explore either the number of knots with an equidistant configuration or simultaneously explore both the locations and the number of knots ([Kang and Jeong, 2023](#)). In this study, our focus is specifically on controlling the number of knots based on the equidistance system, aligning with Bayesian basis selection employed in our proposed approach. A more comprehensive discussion on Bayesian basis selection can be found in [Kang and Jeong \(2023\)](#).

Bayesian basis selection allows for the incorporation of various types of basis functions, including but not limited to the natural cubic spline basis, Fourier basis, Bernstein polynomials, and radial basis functions, among others (e.g., [Kohn et al., 2001](#); [Shen and Ghosal, 2015](#); [Kang and Jeong, 2023](#)). Here, our focus is on the B-spline basis functions. With the equally spaced knot specification, the basic idea of Bayesian basis selection is to choose the optimal number J for the spline approximation $f(\cdot) = \sum_{j=1}^J \theta_j B_j(\cdot)$, where B_j are the B-spline basis terms, by employing an appropriate prior for θ_J . Given the nature of BMS, using an informative prior for θ_J is essential ([Moreno et al., 1998](#)). However, this leads to an informative prior for the height of the function, consequently leading to a lack of invariance in relation to shifts in the target function. To address this concern, a common approach is segregating the global mean term \bar{f} and assigning a flat prior to it with an identifiability assumption on the remaining signal \tilde{f} , that is, $f(\cdot) = \bar{f} + \tilde{f}(\cdot)$ with $\sum_{i=1}^n \tilde{f}(x_i) = 0$ ([Jeong et al., 2022](#)). Utilizing the B-splines, this can be achieved through the use of transformed basis functions represented as $x \mapsto \{1, \tilde{B}_2(x), \dots, \tilde{B}_J(x)\}$, where $\tilde{B}_j(\cdot) = B_j(\cdot) - n^{-1} \sum_{i=1}^n B_j(x_i)$. The transformed basis spans the same spline space as the original B-spline basis due to the sum-to-unity. Letting $\bar{f} = \tilde{\theta}_1$ and $\tilde{f}(\cdot) = \sum_{j=2}^J \tilde{\theta}_j \tilde{B}_j(\cdot)$, $\theta_j \in \mathbb{R}$, $j = 1, \dots, J$, we arrive at the expression $f(\cdot) = \tilde{\theta}_1 + \sum_{j=2}^J \tilde{\theta}_j \tilde{B}_j(\cdot)$ ([Xue, 2009](#); [Jeong et al., 2022](#); [Kang and Jeong, 2023](#); [Wood, 2017](#), Section 4.3).

As stated above, it remains crucial to choose a reasonable prior for $\tilde{\theta}_J = (\tilde{\theta}_2, \dots, \tilde{\theta}_J)^T \in \mathbb{R}^{J-1}$, while also assigning a flat prior to the global mean term to achieve invariance with shifts. Within the basis selection framework, one commonly used prior is Zellner’s g-prior ([Zellner, 1986](#); [Smith](#)

and Kohn, 1996; Kohn et al., 2001; Jeong et al., 2022; Kang and Jeong, 2023),

$$\begin{aligned} \pi(\tilde{\theta}_1) &\propto 1, \\ \tilde{\theta}_J | J, \lambda, \sigma^2 &\sim N_{J-1}(\mathbf{0}, \lambda\sigma^2 n(\tilde{\mathbf{B}}_J^T \tilde{\mathbf{B}}_J)^{-1}), \end{aligned} \tag{4}$$

where $\tilde{\mathbf{B}}_J \in \mathbb{R}^{n \times (J-1)}$ represents the basis matrix with $\tilde{B}_{j+1}(x_i)$ for the (i, j) th element. (A more common representation is to let $g = \lambda n$ for (4) and consider the appropriate value of g that scales the term $(\tilde{\mathbf{B}}_J^T \tilde{\mathbf{B}}_J)^{-1}$ with n , but our parameterization is more straightforward in constructing the proposed method in the subsequent section.) The prior requires a suitable truncation of the support for J to ensure the invertibility of $\tilde{\mathbf{B}}_J^T \tilde{\mathbf{B}}_J$. It is evident that (4) exhibits invariance with respect to shifting and scaling of \mathbf{y} , as well as invariance under an invertible linear transformation of the design matrix (Liang et al., 2008).

It is worth noting that the prior in (4) penalizes deviations from the center $\tilde{f}(\cdot) = f(\cdot) - \bar{f}$ through the term $n^{-1} \tilde{\theta}_J^T \tilde{\mathbf{B}}_J^T \tilde{\mathbf{B}}_J \tilde{\theta}_J$ as a Tikhonov penalty. This term can be approximated by $\|f - \bar{f}\|_2^2 = \int (f(x) - \bar{f})^2 dx$ if the design points are sufficiently regular. Thus, the resulting conditional posterior can be interpreted as

$$-\log \pi(f | \mathbf{y}, J, \lambda, \sigma^2) \approx -\log\text{-likelihood} + \frac{1}{2\lambda\sigma^2} \|f - \bar{f}\|_2^2 + c, \tag{5}$$

for some constant c independent of the coefficients. Therefore, Bayesian basis selection can be viewed as the process of choosing the optimal J while penalizing complex models using the magnitude of $f(\cdot) - \bar{f}$.

The variance parameter σ^2 is assigned an inverse gamma prior, $\sigma^2 \sim \text{IG}(a_\sigma, b_\sigma)$, with $a_\sigma \geq 0$ and $b_\sigma \geq 0$. The convention in the BMS literature is to use an improper prior with $a_\sigma = 0$ and $b_\sigma = 0$ (Liang et al., 2008). Regarding the value of λ , it has been found that choosing a fixed λ may result in the paradoxes of BMS (Liang et al., 2008; Li and Clyde, 2018) and worsen the performance of nonparametric function estimation (Kang and Jeong, 2023). Accordingly, it is frequently advised to assign a prior distribution on λ . One simple yet effective approach is to employ an inverse gamma prior, $\lambda \sim \text{IG}(1/2, 1/2)$ (or $g = \lambda n \sim \text{IG}(1/2, n/2)$) (Zellner and Siow, 1980), which benefits from the semi-conjugacy. Various alternative mixtures of g-priors are available for Bayesian basis selection (Kang and Jeong, 2023), including the beta-prime prior (Maruyama and George, 2011) and the robust prior (Bayarri et al., 2012) for $g = \lambda n$. The prior specification is completed with a prior on J , denoted as $\pi(J)$, which can be chosen as a uniform distribution to benefit from practical considerations or as an exponentially decaying prior to ensure theoretical optimality (Shen and Ghosal, 2015).

Focusing on the g-prior, Bayesian basis selection can be straightforwardly implemented through a closed-form expression of the marginal likelihood of Gaussian regression. It also offers an interesting interpretation in connection with information criteria such as AIC and BIC if λ is appropriately chosen (George and Foster, 2000). Moreover, this method benefits from firmly established asymptotic properties that allow for adaptation to levels of unknown smoothness (Shen and Ghosal, 2015; De Jonge and Van Zanten, 2012; Belitser and Serra, 2014) (The standard theory requires replacing the improper prior with a proper distribution.) However, function estimation is carried out solely by utilizing the given basis terms without any additional penalty on function smoothness. This leads to substantial estimation bias stemming from the approximation

error between the true function and the spline approximation, as BMS often prioritizes identifying parsimonious models solely based on the available data, disregarding the infinite-dimensional nature inherent in the true model. This negative feature is also clear in Figure 1. One potential solution involves controlling both the number and locations of knots to identify a better knot specification (Smith and Kohn, 1996; Denison et al., 1998; DiMatteo et al., 2001). However, this idea is better suited for locally adaptive estimation and can become unnecessarily intricate and time-consuming if the smoothness remains constant over the domain (Kang and Jeong, 2023). In contrast, Bayesian P-splines are relatively free of the bias issue, as they utilize a direct penalty on smoothness with a reasonably large number of knots.

3 Proposed Method

In this section, we present our proposed method, which leverages the synergy between Bayesian P-splines and basis selection through BMS. The cornerstone of our method lies in designing an appropriate prior distribution that effectively integrates the Bayesian P-spline prior in (2) with the model selection prior in (4). We provide a computationally efficient MCMC algorithm to obtain the model-averaged posterior distribution.

3.1 Prior Specification

The success of the proposed approach relies on effectively harmonizing the two prior distributions. One notable issue arises from the fact that these two prior distributions apply to different parameterizations: the P-spline prior in (2) is concerned with the coefficients of the original B-spline basis functions $x \mapsto \{B_1(x), B_2(x), \dots, B_J(x)\}$, while the prior in (4) pertains to the coefficients of the transformed basis functions $x \mapsto \{1, \tilde{B}_2(x), \dots, \tilde{B}_J(x)\}$. In order to combine them on an equivalent basis, it is advantageous to express both prior distributions in terms of the same coefficients. To this end, the following proposition presents the prior distribution derived from (2), which is associated with the coefficients of the transformed basis terms as constructed in (4). The proof is given in Appendix C.

Proposition 1. *The Bayesian P-spline prior for $(\tilde{\theta}_1, \tilde{\theta}_J)$, derived from the original prior in (2), is given by*

$$\begin{aligned} \pi(\tilde{\theta}_1) &\propto 1, \\ \pi(\tilde{\theta}_J \mid \lambda) &\propto \frac{1}{\lambda^{\text{rank}(\tilde{\mathbf{P}}_J)/2}} \exp\left(-\frac{1}{2\lambda} \tilde{\theta}_J^T \tilde{\mathbf{P}}_J \tilde{\theta}_J\right), \end{aligned} \tag{6}$$

where $\tilde{\mathbf{P}}_J = \tilde{\mathbf{D}}_J^T \tilde{\mathbf{D}}_J \in \mathbb{R}^{(J-1) \times (J-1)}$ for $\tilde{\mathbf{D}}_J \in \mathbb{R}^{(J-2) \times (J-1)}$ the matrix constructed by removing the first column of \mathbf{D}_J .

The interpretation in (3) remains unchanged for the modified prior in (6). Observe that both the model selection prior in (4) and the modified P-spline prior in (6) impose a flat improper prior on the global mean parameter. For the remaining coefficients associated with the centered signal, these priors utilize a proper Gaussian distribution and an improper distribution with density proportional to a singular normal distribution, respectively. Although the prior in (6) lacks scale

invariance for the observations and requires the standardization of \mathbf{y} as discussed in Section 2.1, it can be readily adapted by incorporating σ^2 in the exponent. Motivated by these observations, we propose the following fused prior distribution on $(\tilde{\theta}_1, \tilde{\theta}_J)$,

$$\begin{aligned} \tilde{\theta}_1 | \sigma^2 &\sim \text{N}(0, \sigma^2 \kappa^2), \\ \tilde{\theta}_J | J, \sigma^2, \lambda, \tau &\sim \text{N}_{J-1} \left(\mathbf{0}, \lambda \sigma^2 \left((1 - \tau) \tilde{\mathbf{P}}_J + \tau n^{-1} \tilde{\mathbf{B}}_J^T \tilde{\mathbf{B}}_J \right)^{-1} \right), \end{aligned} \quad (7)$$

where $\kappa > 0$ is a fixed constant, while $\lambda > 0$ and $\tau \in (0, 1)$ are parameters that require suitable prior distributions. Observe that the covariance matrix is invertible since we assume that $\tilde{\mathbf{B}}_J^T \tilde{\mathbf{B}}_J$ is positive definite. Choosing a sufficiently large κ is satisfactory, as it causes the prior to mimic a flat prior for the global mean, ensuring that it remains uninfluenced by other coefficients. Alternatively, one could employ the flat prior $\pi(\tilde{\theta}_1) \propto 1$ from a practical perspective. However, the proper proxy in (7) is useful for deriving theoretical results, while yielding a posterior distribution that is essentially comparable.

Given the expressions in (3) and (5), the resulting conditional posterior with the proposed prior in (7) can be interpreted as

$$-\log \pi(f | \mathbf{y}, J, \lambda, \sigma^2) \approx -\log\text{-likelihood} + \frac{1}{2\lambda\sigma^2} \left\{ (1 - \tau) \|f''\|_2^2 + \tau \|f - \bar{f}\|_2^2 \right\} + c,$$

for some constant c independent of the coefficients. Hence, the prior in (7) can be viewed as imposing a penalty through a convex combination of the two penalty terms. Instead of relying on a single penalty term, the prior in (7) thus makes use of the combined effectiveness of both terms.

The weight parameter $\tau \in (0, 1)$ serves as a means to strike a balance between the two penalty terms, effectively determining the relative importance of penalization versus model selection. If $\tau \rightarrow 0$, the prior in (7) is viewed as a proxy of the P-spline prior in (6) with an additional hierarchy on σ^2 . On the other hand, if $\tau \rightarrow 1$, the prior approaches to the model selection prior in (4). Given its possible range, a natural prior for τ is a uniform distribution on $(0, 1)$ or a beta distribution. Although this reasonably works in empirical studies, our theoretical analysis necessitates a prior with an exponentially decaying tail towards zero to ensure the positive definiteness of the covariance matrix with a high prior probability. Note that a standard beta distribution does not satisfy this requirement, as it exhibits polynomial tails. As a practical solution, we truncate a uniform prior on $(\delta, 1 - \delta)$ with a small $\delta > 0$.

Combined with τ , the dispersion parameter λ plays similar roles in Bayesian P-splines and Bayesian basis selection. More precisely, the factor $\lambda/(1 - \tau)$ controls the smoothness of the function through $\tilde{\mathbf{P}}_J$, while the term λ/τ determines deviations from the center through $n^{-1} \tilde{\mathbf{B}}_J^T \tilde{\mathbf{B}}_J$. An inverse gamma prior on λ , which appears to be the most natural due to its semi-conjugacy, only provides a polynomial tail on the right side. Since our theory for optimal posterior contraction requires a prior distribution with an exponentially decaying tail, we employ an exponential prior distribution for λ , that is, $\lambda \sim \text{Exp}(c_\lambda)$, where $c_\lambda > 0$ is a rate parameter. While other distributions with exponential tails can also be used, an exponential prior is particularly advantageous when constructing an MCMC algorithm with slice sampling (Neal, 2003); see Section 3.2 for more details. As an additional benefit, we observe that an exponential prior on λ leads to a

slight improvement in mixing of the MCMC algorithm when compared to using an inverse gamma prior. This improvement stems from a potential issue of numerical identifiability between λ and J , as both parameters contribute to penalizing the function. A prior distribution with a thinner tail resolves this issue by constraining λ to smaller values.

It is essential to employ an appropriate prior for J in order to achieve optimal posterior contraction. Similar to the context of Bayesian basis selection, a prior with an exponentially decaying property can effectively penalize large models (Shen and Ghosal, 2015). In line with this approach, we utilize a truncated geometric prior, $\pi(J) \propto \nu^J$, $J = 4, 5, \dots, n$, where $\nu \in (0, 1)$ is a fixed constant. The support truncation to $\{4, 5, \dots, n\}$ ensures both the full column rank of $\tilde{\mathbf{B}}_J$ and the minimal spline model dimension as a cubic degree. Choosing ν close to 1 results in the prior closely resembling a discrete uniform distribution, making it weakly informative. Nonetheless, it has come to our attention that a slightly smaller value enhances numerical stability while maintaining essentially comparable estimation performance. Therefore, we set $\nu = 0.9$ as the default value.

For the variance parameter σ^2 , we use a conjugate inverse gamma prior, $\sigma^2 \sim \text{IG}(a_\sigma, b_\sigma)$, with $a_\sigma \geq 0$ and $b_\sigma \geq 0$. While a practical perspective may suggest using the Jeffreys prior with $a_\sigma = 0$ and $b_\sigma = 0$, our theoretical analysis necessitates a proper prior with $a_\sigma > 0$ and $b_\sigma > 0$. Choosing small values for $a_\sigma > 0$ and $b_\sigma > 0$ is a reasonable alternative to the noninformative prior.

Remark 1. Instead of combining the two penalty terms, one might prefer to extend Bayesian P-splines by incorporating basis selection solely through the penalty term involving $\tilde{\mathbf{P}}_J$. Furthermore, one might also consider penalizing the function using both penalties simultaneously without basis selection. We include these approaches as competitors of the proposed method in our simulation study in Section 5. Our results demonstrate that the proposed method outperforms these alternative ideas. See Section 5 for details.

3.2 Efficient Monte Carlo Sampling Algorithm

We present an efficient MCMC algorithm for sampling from the joint posterior distribution $\pi(J, \sigma^2, \tilde{\theta}_1, \tilde{\theta}_J, \lambda, \tau | \mathbf{y})$. Our carefully designed prior distribution enables sampling from the posterior distribution to be straightforward and easily implementable. Once the MCMC draws are collected, one can produce the model-averaged posterior of any functional of f , for example, pointwise evaluations at specific values or credible bands of the function. The following is a blocked Gibbs sampler that alternates between the full conditionals of $(J, \sigma^2, \tilde{\theta}_1, \tilde{\theta}_J)$, λ , and τ .

- (i) Draw J from $\pi(J | \lambda, \tau, \mathbf{y}) \propto \pi(J) p(\mathbf{y} | J, \lambda, \tau)$, where $p(\mathbf{y} | J, \lambda, \tau)$ is the marginal likelihood given by

$$p(\mathbf{y} | J, \lambda, \tau) \propto |\mathbf{I}_{J-1} - \boldsymbol{\Omega}_{J, \lambda, \tau}^{-1} \tilde{\mathbf{B}}_J^T \tilde{\mathbf{B}}_J|^{1/2} \times \left(b_\sigma + \frac{1}{2} \left[\mathbf{y}^T \mathbf{y} - \frac{(\mathbf{y}^T \mathbf{1}_n)^2}{n + \kappa^2} - \mathbf{y}^T \tilde{\mathbf{B}}_J \boldsymbol{\Omega}_{J, \lambda, \tau}^{-1} \tilde{\mathbf{B}}_J^T \mathbf{y} \right] \right)^{-(a_\sigma + n/2)},$$

with $\boldsymbol{\Omega}_{J, \lambda, \tau} = (1 - \tau) \lambda^{-1} \tilde{\mathbf{P}}_J + (n + \tau / \lambda) n^{-1} \tilde{\mathbf{B}}_J^T \tilde{\mathbf{B}}_J$. We draw J using the Metropolis-Hastings algorithm. Given the current J , a proposal is either $J + 1$ or $J - 1$ with equal probabilities.

(ii) Draw σ^2 from $\pi(\sigma^2|J, \lambda, \tau, \mathbf{y})$, where

$$\sigma^2|J, \lambda, \tau, \mathbf{y} \sim \text{IG}\left(a_\sigma + \frac{n}{2}, b_\sigma + \frac{1}{2}\left[\mathbf{y}^T \mathbf{y} - \frac{(\mathbf{y}^T \mathbf{1}_n)^2}{n + \kappa^2} - \mathbf{y}^T \tilde{\mathbf{B}}_J \boldsymbol{\Omega}_{J, \lambda, \tau}^{-1} \tilde{\mathbf{B}}_J^T \mathbf{y}\right]\right).$$

(iii) Draw $(\tilde{\theta}_1, \tilde{\boldsymbol{\theta}}_J)$ from $\pi(\tilde{\theta}_1, \tilde{\boldsymbol{\theta}}_J|\sigma^2, J, \lambda, \tau, \mathbf{y})$, where

$$\begin{aligned} \tilde{\theta}_1|\sigma^2, \mathbf{y} &\sim \text{N}(\mathbf{y}^T \mathbf{1}_n / (n + \kappa^{-2}), \sigma^2 / (n + \kappa^{-2})), \\ \tilde{\boldsymbol{\theta}}_J|\sigma^2, J, \lambda, \tau, \mathbf{y} &\sim \text{N}_{J-1}\left(\boldsymbol{\Omega}_{J, \lambda, \tau}^{-1} \tilde{\mathbf{B}}_J^T \mathbf{y}, \sigma^2 \boldsymbol{\Omega}_{J, \lambda, \tau}^{-1}\right). \end{aligned}$$

(iv) Draw λ from $\pi(\lambda|J, \tau, \sigma^2, \tilde{\theta}_1, \tilde{\boldsymbol{\theta}}_J, \mathbf{y})$. This can be easily achieved using slice sampling, which involves drawing an auxiliary variable γ ,

$$\begin{aligned} \gamma &\sim \text{Unif}(0, h(\lambda; c_\lambda)), \\ \lambda|\gamma, J, \tau, \sigma^2, \tilde{\theta}_1, \tilde{\boldsymbol{\theta}}_J, \mathbf{y} &\sim \text{IG}_{(0, h^{-1}(\gamma; c_\lambda))}\left(\frac{J-3}{2}, \frac{1}{2\sigma^2} \tilde{\boldsymbol{\theta}}_J^T \left((1-\tau)\tilde{\mathbf{P}}_J + \tau n^{-1} \tilde{\mathbf{B}}_J^T \tilde{\mathbf{B}}_J\right) \tilde{\boldsymbol{\theta}}_J\right), \end{aligned}$$

where $h(\cdot; c_\lambda)$ denotes the exponential density with a rate parameter c_λ and IG_A represents an inverse gamma distribution truncated to A . Observe that h^{-1} is available in a closed form. The details of the derivation are provided in Appendix A.

(v) Draw τ from $\pi(\tau|J, \lambda, \sigma^2, \tilde{\theta}_1, \tilde{\boldsymbol{\theta}}_J, \mathbf{y}) \propto \pi(\tau)\pi(\tilde{\boldsymbol{\theta}}_J|J, \sigma^2, \lambda, \tau)$. This can be efficiently achieved through grid sampling using that

$$\begin{aligned} \log \pi(\tilde{\boldsymbol{\theta}}_J|J, \sigma^2, \lambda, \tau) &= \frac{1}{2} \sum_{k=1}^{J-1} \log\left(1 + \frac{(1-\tau)n}{\tau} \rho_k\left(\left(\tilde{\mathbf{B}}_J^T \tilde{\mathbf{B}}_J\right)^{-1} \tilde{\mathbf{P}}_J\right)\right) \\ &\quad + \frac{J-1}{2} \log \tau - \frac{1-\tau}{2\lambda\sigma^2} \tilde{\boldsymbol{\theta}}_J^T \tilde{\mathbf{P}}_J \tilde{\boldsymbol{\theta}}_J - \frac{\tau}{2n\lambda\sigma^2} \tilde{\boldsymbol{\theta}}_J^T \tilde{\mathbf{B}}_J^T \tilde{\mathbf{B}}_J \tilde{\boldsymbol{\theta}}_J + c, \end{aligned} \tag{8}$$

where $\rho_k(\cdot)$ denotes the k th eigenvalue of a matrix in a decreasing order and c is a constant independent of τ . The sampling is highly efficient since it necessitates matrix multiplications and eigenvalue computations only once during the evaluation of the log density at grid points of τ . The details are provided in Appendix A.

4 Theoretical Analysis

In this section, we investigate a theoretical aspect of the proposed method. More specifically, we establish that our proposed method for nonparametric regression achieves the optimal posterior contraction rate in the minimax sense up to a logarithmic factor. Coupled with a given semi-metric for the parameter, a posterior contraction rate characterizes the speed at which the posterior distribution contracts towards the true parameter of the data distribution. We show that the proposed method is adaptive within the Bayesian framework, as it achieves the nearly optimal rate without requiring prior knowledge about the smoothness parameter of the true function. Below, we outline the conditions required to achieve the adaptive posterior contraction.

(A1) The true function f_0 for data generation belongs to the α -Hölder space $\mathcal{H}^\alpha([0, 1]) = \{f : [0, 1] \rightarrow \mathbb{R}; \|f\|_{\mathcal{H}^\alpha} < \infty\}$ with $\alpha \in (0, l + 1]$, where

$$\|f\|_{\mathcal{H}^\alpha} = \max_{0 \leq k \leq \lfloor \alpha \rfloor} \sup_{x \in [0, 1]} |f^{(k)}(x)| + \sup_{x, y \in [0, 1]: x \neq y} \frac{|f^{(\lfloor \alpha \rfloor)}(x) - f^{(\lfloor \alpha \rfloor)}(y)|}{|x - y|^{\alpha - \lfloor \alpha \rfloor}}.$$

(A2) The true variance parameter σ_0^2 for data generation satisfies $c^{-1} \leq \sigma_0^2 \leq c$ for some constant $c > 1$.

(A3) For the fixed design points $x_i, i = 1, \dots, n$, there exists a distribution function G such that

$$\|G_n - G\|_\infty = o(n^{-1/(2\alpha+1)}(\log n)^{-2\alpha/(2\alpha+1)}),$$

where $G_n(\cdot) = n^{-1} \sum_{i=1}^n \mathbb{1}\{\cdot \leq x_i\}$ is the empirical distribution function of $x_i, i = 1, \dots, n$.

Assumption (A1) is conventionally made in the literature on nonparametric regression, and it is well known that the corresponding minimax rate for function estimation is $n^{-\alpha/(2\alpha+1)}$ (Stone, 1982). Assumption (A2) is obviously minor and imposes that the true σ_0^2 belongs to a compact subset of $(0, \infty)$. Assumption (A3) is common in the relevant literature (Shen et al., 1998; Yoo and Ghosal, 2016; Xiao, 2019). It means that the design points are sufficiently regularly distributed in terms of their empirical distribution. This assumption is mostly required to guarantee that the minimum and maximum eigenvalues of $n^{-1} \mathbf{B}_J^T \mathbf{B}_J$ have an asymptotic order of J^{-1} if $J \lesssim n^{1/(2\alpha+1)}(\log n)^{2\alpha/(2\alpha+1)}$ (Lemma 3). Although the assumption is nontrivial, it is often satisfied under mild situations. For example, the discrete uniform design, $x_i = (i-1)/(n-1), i = 1, \dots, n$, satisfies (A3) with G being the uniform distribution on $[0, 1]$ for any $\alpha > 0$. If x_i are independently generated from the distribution G , (A3) is satisfied with probability tending to one as soon as $\alpha > 1/2$ by Donsker's theorem. We present results on posterior contraction rates based on fixed design points. The random design case can be treated by conditioning on $x_i, i = 1, \dots, n$.

The following theorem formally characterizes the posterior contraction rate of the proposed method with respect to a suitably defined semi-metric between (f, σ) and the truth (f_0, σ_0) . The theorem shows that the proposed method exhibits the posterior contraction rate that is minimax-optimal up to a logarithmic factor. The theorem holds uniformly over $f_0 \in \mathcal{H}^\alpha([0, 1])$ with $\alpha \in (0, l + 1]$.

Theorem 1. *Suppose that (A1)–(A3) hold for the model in (1) with the prior distribution specified in Section 3.1. For every $M_n \rightarrow \infty$, the posterior distribution satisfies*

$$\mathbb{E}_0 \Pi \left(\|f - f_0\|_n + |\sigma - \sigma_0| > M_n n^{-\alpha/(2\alpha+1)} (\log n)^{1/(2\alpha+1)+1} \mid \mathbf{y} \right) \rightarrow 0,$$

where \mathbb{E}_0 is the expectation operator under the true measure with f_0 and σ_0^2 .

The proof is provided in Appendix B. Here we discuss a brief outline of the proof approach. Our proof builds upon the theory of posterior contraction with a testing approach (Ghosal et al., 2000; Ghosal and van der Vaart, 2007, 2017). In essence, this approach requires the existence of a test function with exponentially small errors concerning the semimetric used to measure the closeness of the parameters. If σ_0^2 is known, it is well known that a test can be constructed

using the likelihood ratio test (Ghosal and van der Vaart, 2007). However, in scenarios where σ_0^2 is unknown, we encounter a lack of readily available references, despite the availability of a test function within a more intricate framework that extends far beyond our current context (Ning et al., 2020; Jeong and Ghosal, 2021). Therefore, we derive a local test function for small segments within a sieve, as outlined in Lemma 1. Combined with an entropy bound measured by a covering number, this, in turn, establishes a global test function with exponentially small errors (Ghosal et al., 2000). Moreover, despite its practical convenience, using an inverse gamma prior for σ^2 with a hierarchical prior on the coefficients introduces some difficulties in theoretical analysis. To elaborate further, such a prior leads to the marginal prior for the coefficients following a multivariate t -distribution with polynomial tails. Priors with heavy tails pose challenges in achieving Bayesian adaptation to the unknown smoothness because of insufficient decay of the prior probability of a sieve (Shen and Ghosal, 2015; Agapiou and Castillo, 2023). We tackle this issue by directly examining the marginal posterior distribution of σ^2 ; see Lemma 2.

Remark 2. Assumption (A3) can be removed if a small positive definite matrix is added to the covariance matrix of (7) to ensure the positive definiteness regardless of n . However, to avoid introducing such an artificial modification in the prior, we retain Assumption (A3) as one of the requirements for the main results. Nonetheless, it is worth noting that this assumption is quite mild and typically holds in common scenarios.

Remark 3. It is evident that a geometric prior on J satisfies $-\log \pi(J) \asymp J$. A close investigation of the proof reveals that a prior distribution satisfying $-\log \pi(J) \asymp J \log J$, such as a Poisson prior (Shen and Ghosal, 2015), improves the rate in Theorem 1 up to $n^{-\alpha/(2\alpha+1)}(\log n)^{1/(2\alpha+1)}$. Given the immediacy of a geometric prior, we choose not to pursue this minor improvement of the logarithmic term.

5 Simulation Study

5.1 Simulation Setting

In this section, we perform a series of simulation experiments to assess the effectiveness of the proposed method. We will compare the performance of our proposed method with other nonparametric regression approaches. We consider three distinct test functions, $f_j : [0, 1] \rightarrow \mathbb{R}$, $j = 1, 2, 3$, defined as follows:

$$\begin{aligned} f_1(x) &= \exp(x), \\ f_2(x) &= 1 + \sin(2\pi x), \\ f_3(x) &= \frac{\phi_{0.3,0.1}(x) - \phi_{0.7,0.1}(x)}{3} + \frac{2e^{100(x-1/2)}}{3(1 + e^{100(x-1/2)})}, \end{aligned}$$

where $\phi_{\mu,\sigma}$ is the density of a normal distribution with mean μ and standard deviation σ . These functions are listed in increasing order of complexity, with f_1 being the simplest and f_3 the most intricate. The functions are visualized as blue dashed lines in Figure 1 (the top is f_1 , the middle is f_2 , and the bottom is f_3). For each test function, we consider six simulation

scenarios with combinations of $\sigma^2 \in \{0.1^2, 0.5^2\}$ and $n \in \{200, 500, 1000\}$. The design points x_i are independently generated from the uniform distribution on $(0, 1)$.

We will compare the proposed method with several competing approaches, including Bayesian P-splines and Bayesian basis selection. These competitors are chosen to consist of the main components of the proposed method. Below, we enumerate the competitors chosen for comparison under our simulation scenarios.

- *Penalized Splines* (PS30 and PS60). Frequentist penalized B-splines (Eilers and Marx, 1996) are compared to the proposed method. The penalized log-likelihood has the form in (3). We optimize the smoothing parameter using generalized cross-validation to minimize the MSE (Wahba, 1977). This approach can also be seen within a semi-Bayesian framework with an optimized hyperparameter. Once the smoothing parameter is chosen, the pointwise estimator of f follows a normal distribution, allowing for direct calculation of pointwise confidence bands. We refer to the method with 30 and 60 interior knots as PS30 and PS60, respectively.
- *Bayesian P-Splines* (BPS30 and BPS60). We consider Bayesian P-splines as outlined in Section 2.1. Following the recommendation by Brezger and Lang (2006), we set $a_\lambda = b_\lambda = 0.01$ for the prior of λ . The Jeffreys prior is used for σ^2 , that is, $a_\sigma = b_\sigma = 0$. We refer to the method with 30 and 60 interior knots as BPS30 and BPS60, respectively.
- *Bayesian Twofold-Penalty* (BTP30 and BTP60). We include an additional competitive method that incorporates both types of penalties without basis selection. This approach can be implemented by fixing a large number of knots while penalizing the coefficients through the proposed prior in (7). The incorporation of this method aims to clarify the effectiveness of model selection in the proposed approach. As the method relies solely on the penalization of the coefficients, we choose $a_\lambda = b_\lambda = 0.01$ in line with the context of penalized splines. This approach is abbreviated as BTP30 and BTP60 with 30 and 60 interior knots, respectively.
- *Bayesian Basis Selection* (BBS-ZS, BBS-BP, and BBS-R). Bayesian basis selection, described in Section 2.2, is considered for comparison. Based on the convention in the BMS literature (Liang et al., 2008), we compare the Zellner-Siow prior (Zellner and Siow, 1980), the beta-prime prior (Maruyama and George, 2011), and the robust prior (Bayarri et al., 2012) to explore potential differences in model selection prior distributions. The Jeffreys prior is used for σ^2 . These methods are abbreviated as BBS-ZS, BBS-BP, and BBS-R, respectively.
- *Bayesian P-Splines with Basis Selection* (BPSwBS). We consider Bayesian P-splines with basis selection instead of specifying a fixed number of knots. This approach can be achieved by replacing the covariance matrix for $\tilde{\boldsymbol{\theta}}_J$ in (7) with $\lambda\sigma^2(\tilde{\mathbf{P}}_J + \eta\mathbf{I}_{J-1})^{-1}$, where $\eta > 0$ is a small constant. The inclusion of the term $\eta\mathbf{I}_{J-1}$ ensures that the resulting prior distribution remains proper while maintaining a similar role to the P-spline prior. We choose $\lambda \sim \text{IG}(1/2, 1/2)$ (the Zellner-Siow prior) based on the BMS context, yet using $\lambda \sim \text{IG}(0.01, 0.01)$ within the P-splines framework yields marginal differences in performance. This method is referred to as BPSwBS.

Methods	$\ f''\ _2$ -penalty	$\ f - \hat{f}\ _2$ -penalty	Basis selection
PS30 and PS60	✓	-	-
BPS30 and BPS60	✓	-	-
BTP30 and BTP60	✓	✓	-
BBS-ZS, BBS-BP, and BBS-R	-	✓	✓
BPSwBS	✓	-	✓
Proposed method	✓	✓	✓

Table 1: Summary of the key components of the competitors and the proposed method.

Alongside the aforementioned competitors, we implement the proposed method as described in Section 3. For the prior for λ , we choose $\text{Exp}(c_\lambda)$ with $c_\lambda = 0.315$ to closely match its median with that of $\text{IG}(1/2, 1/2)$. We also tested $c_\lambda = 0.1$ and $c_\lambda = 0.5$, but observed little difference in performance. Although our theoretical analysis requires a proper prior, we employ the Jeffreys prior for σ^2 in our numerical experiments. We set $\kappa = 10^7$ for the proposed prior in (7). Furthermore, we choose $\nu = 0.9$ for the proposed method, as well as for other approaches that perform basis selection (BBS-ZS, BBS-BP, BBS-R, and BPSwBS). The key components of the competitors and the proposed method are summarized in Table 1.

5.2 Results

For each method within every simulation scenario, we generate 500 replications of datasets. Based on these replications, we evaluate the MSEs and the coverage probabilities of the pointwise credible (or confidence) bands. We also calculate the MSEs of the first and second derivatives to assess the local variability and smoothness of the estimated functions. All results are based on MCMC draws of size 10000 after suitable burn-in periods.

Figure 2 and Figure 3 illustrate the estimated MSEs and 95% coverage probabilities, respectively. Frequentist penalized splines (PS30 and PS60) exhibit satisfactory (though not the best) performance in terms of the MSE, as they are fitted by directly minimizing it using generalized cross-validation. However, they frequently struggle to correctly quantify uncertainty through the 95% pointwise confidence bands. Bayesian P-splines (BPS30 and BPS60) exhibit a relatively poor performance for estimating f_1 and f_2 , which arises from potential overfitting as discussed in Section 2.1 (see Figure 1). Moreover, Bayesian P-splines tend to overestimate coverage probabilities in almost all cases; the estimated probabilities are often close to 100% rather than 95%. Another substantial drawback is that the performance of Bayesian P-splines is significantly influenced by the chosen number of knots, whereas frequentist penalized splines are less sensitive. Bayesian basis selection (BBS-ZS, BBS-BP, and BBS-R) performs reasonably well in estimating f_1 and f_2 in terms of the MSE but shows substantially inferior performance in estimating f_3 compared to other methods. This is attributed to the susceptibility of BBS to underfitting resulting from model misspecification (see Figure 1). Furthermore, it exhibits incorrect quantification of uncertainty, as reflected in 95% coverage probabilities. The coverage performance is particularly lacking for f_2 and f_3 . Observe that incorporating the twofold penalty (BTP30 and BTP60) does not prove effective in mitigating the drawbacks of Bayesian P-splines. Compared to the competitors, the

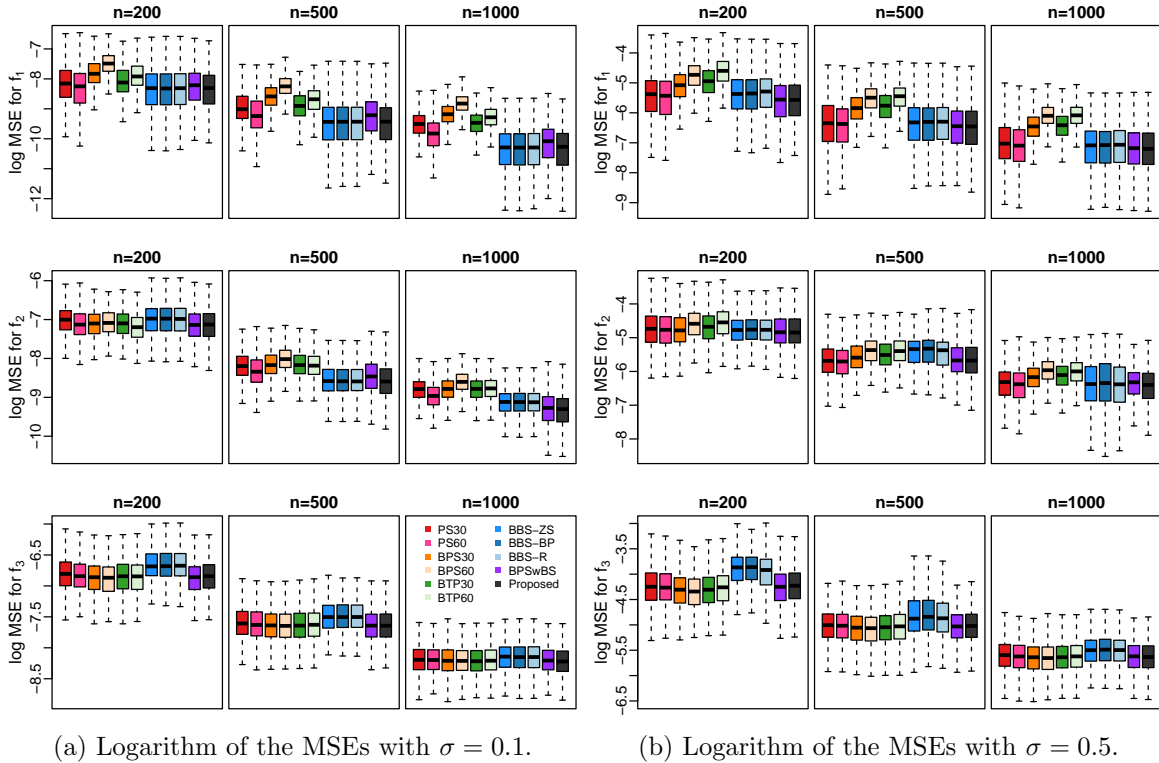
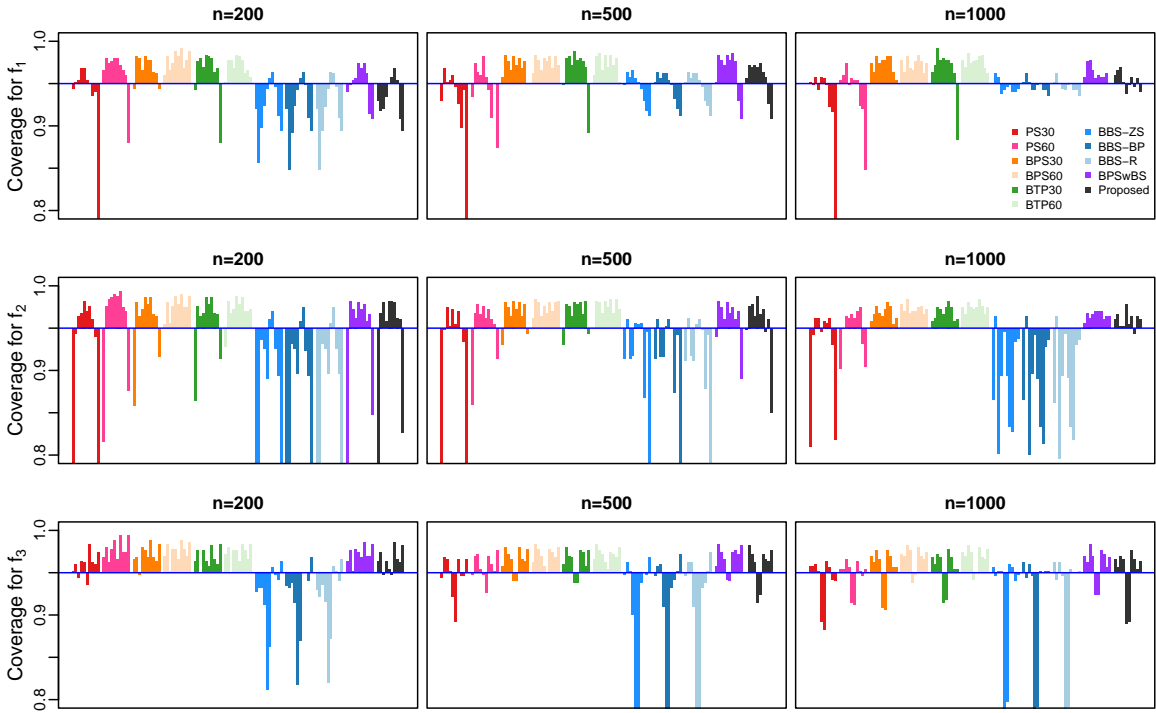


Figure 2: Logarithm of the MSEs for the test functions f_1 , f_2 , and f_3 , obtained from 500 replicated datasets.

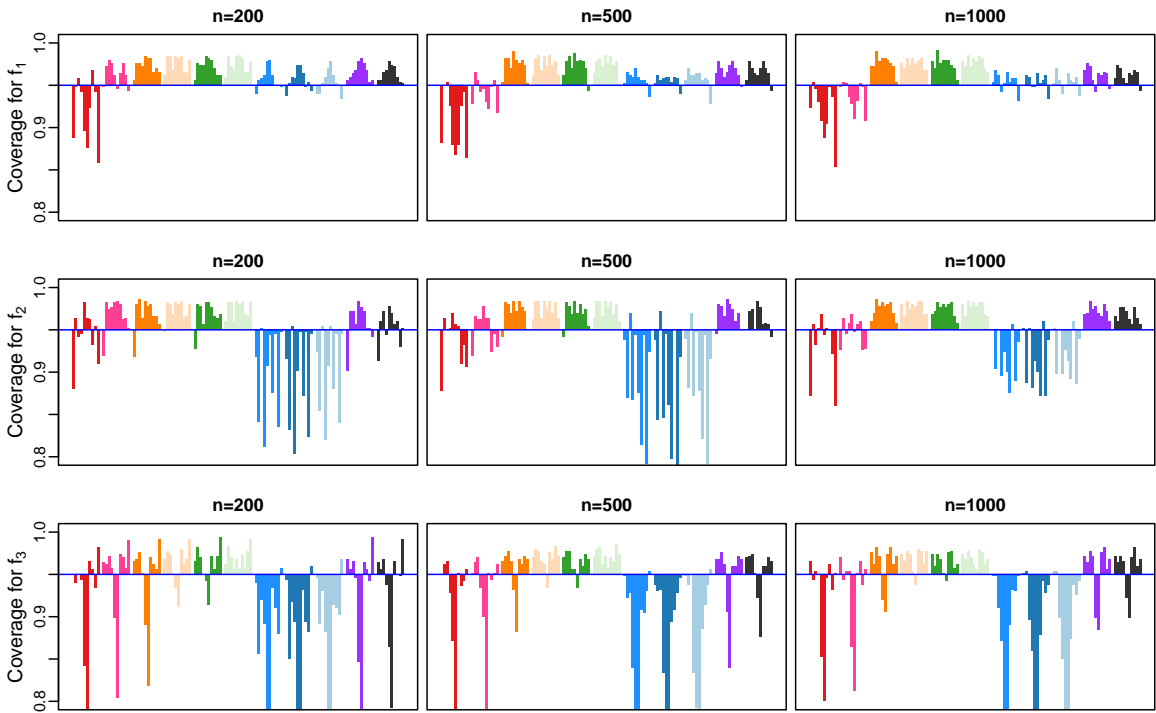
proposed method performs excellently in terms of both the MSE and coverage probability. BPSwBS exhibits similar performance to the proposed method, with the latter slightly outperforming by achieving smaller MSEs and coverage probabilities closer to 95%.

Figure 4 and Figure 5 display the estimated MSEs of the first and second derivatives of the target functions, respectively. As illustrated in Figure 1, potential overfitting leads to significant underperformance of Bayesian P-splines and their variants in estimating the first and second derivatives for f_1 and f_2 , whereas the smoothness of f_3 is correctly accounted for. On the contrary, Bayesian basis selection (BBS-ZS, BBS-BP, and BBS-R) substantially outperforms penalized splines for estimating the derivatives of f_1 and f_2 , albeit showing inferior performance for f_3 due to bias induced by model misspecification (see Figure 1). In comparison to the other methods, the proposed method demonstrates outstanding performance in accurately estimating the first and second derivatives of all test functions, performing similarly to Bayesian basis selection for f_1 and f_2 , and closely aligning with Bayesian P-splines for f_3 . While BPSwBS also exhibits reasonable effectiveness, the proposed method generally outperforms it.

The complexity of models involving basis selection is primarily influenced by the dimension J . More complex models may lead to computational inefficiency, as one iteration of the MCMC algorithm involves $O(J^3)$ operations due to matrix determinant and inversion. Hence, if competing methods exhibit similar performance, it is advisable to use the approach that yields a sparser configuration of knots. In particular, as BPSwBS exhibits the closest performance to the proposed

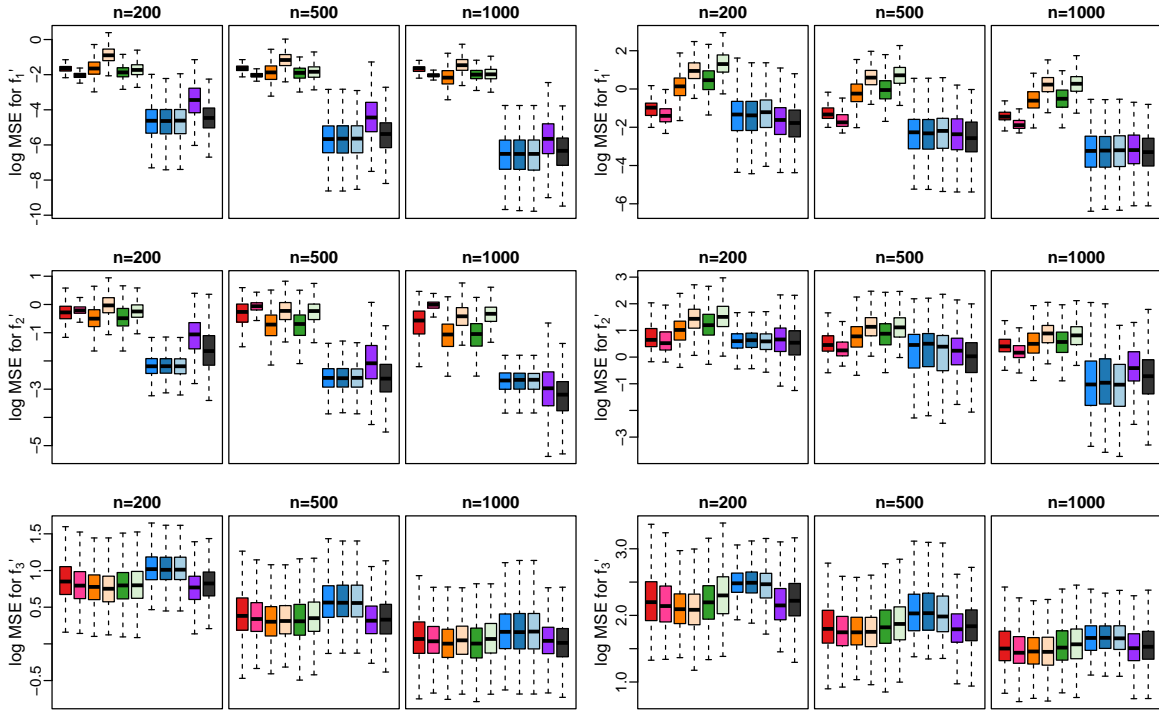


(a) Coverage probabilities of the 95% pointwise credible (or confidence) bands with $\sigma = 0.1$.



(b) Coverage probabilities of the 95% pointwise credible (or confidence) bands with $\sigma = 0.5$.

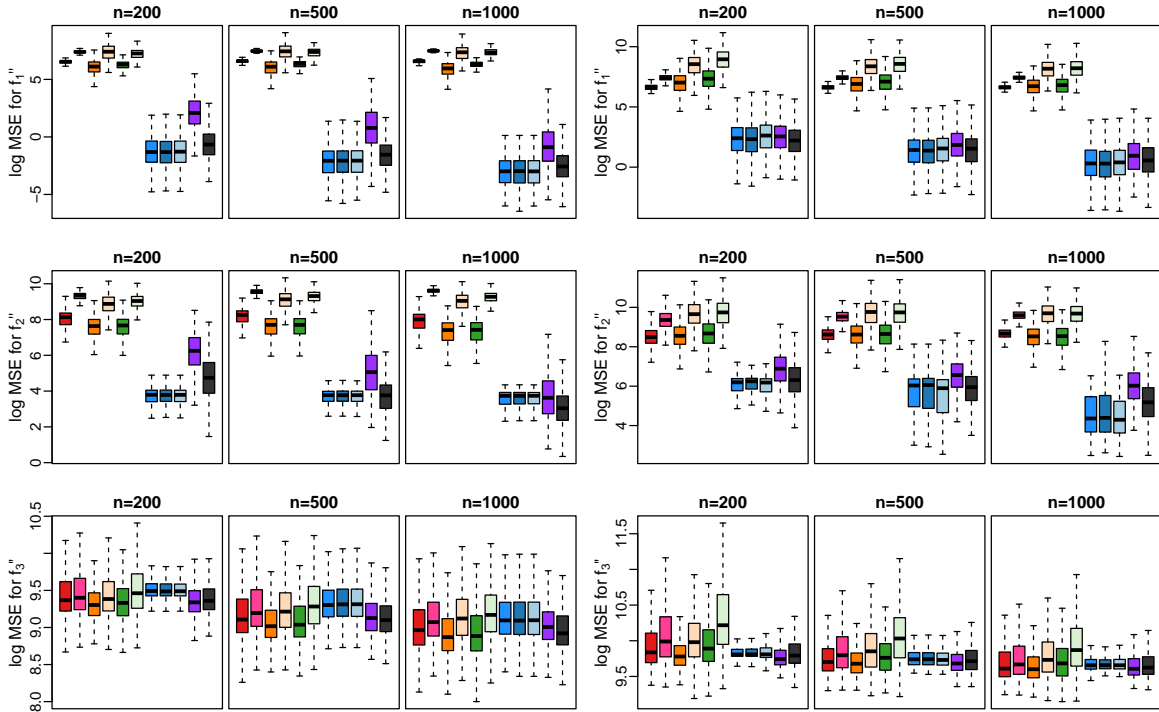
Figure 3: Coverage probabilities of the 95% pointwise credible (or confidence) bands for the test functions f_1 , f_2 , and f_3 , obtained from 500 replicated datasets. Each bar for each method represents the deviation of the pointwise coverage probability from 95% at $x \in \{0.05, 0.15, 0.25, \dots, 0.95\}$.



(a) Logarithm of the MSEs for f' with $\sigma = 0.1$. (b) Logarithm of the MSEs for f' with $\sigma = 0.5$.

Figure 4: Logarithm of the MSEs for the first derivatives of the test functions f_1 , f_2 , and f_3 , obtained from 500 replicated datasets with domain truncation to $(0.01, 0.99)$ to eliminate erratic behavior at the boundaries. The color key is the same as in Figure 2 and Figure 3.

method among the competitors, it is particularly interesting to compare the posterior distribution of J between the two methods. Figure 6 shows the posterior mean of J for each method across the 500 replications. The simulation results show that the basis selection methods (BBS-ZS, BBS-BP, and BBS-R) produce similarly small posterior means of J . While this suggests that Bayesian basis selection may be more efficient than the proposed method, previous simulation summaries indicate that its performance lags significantly behind the proposed method in terms of both the MSE and coverage probability. A more interesting comparison lies between BPSwBS and the proposed method. The figure illustrates that BPSwBS consistently requires more basis terms for effective regularization of the target functions. This aligns with intuition, as BPSwBS achieves regularization through an additional penalty on the second derivatives, while Bayesian basis selection determines regularity solely based on the knot configuration. In contrast, the proposed method tends to favor sparser models by incorporating the basis selection prior into the modeling framework along with the P-spline prior, leading to more efficient computation with its smaller posterior mean of J . The implications become more evident as the required J increases, particularly in scenarios such as multivariate nonparametric regression as discussed in Section 7.



(a) Logarithm of the MSEs for f'' with $\sigma = 0.1$. (b) Logarithm of the MSEs for f'' with $\sigma = 0.5$.

Figure 5: Logarithm of the MSEs for the second derivatives of the test functions f_1 , f_2 , and f_3 , obtained from 500 replicated datasets with domain truncation to $(0.01, 0.99)$ to eliminate erratic behavior at the boundaries. The color key is the same as in Figure 2 and Figure 3.

6 Application to the Triceps Dataset

In this section, we employ the proposed method on the triceps dataset (Cole and Green, 1992), which is accessible through the R package `MultiKink`. The dataset consists of the logarithm of the triceps thickness and the age of $n = 892$ female respondents. We use the logarithm of the triceps as the response variable and the age of respondents as the predictor variable for the model in (1).

Figure 7 shows the pointwise posterior mean of the regression function and the 95% pointwise credible band for every method discussed in Section 5. In this example, frequentist penalized splines (PS30 and PS60) and Bayesian basis selection with the Zellner-Siow prior (BBS-ZS) exhibit erratic behavior, possibly attributable to the irregular design points and heteroscedasticity. In contrast, Bayesian P-splines (BPS30 and BPS60) and Bayesian basis selection with the remaining priors (BBS-BP and BBS-R) provide more reasonable fittings. The proposed method performs similarly to the latter.

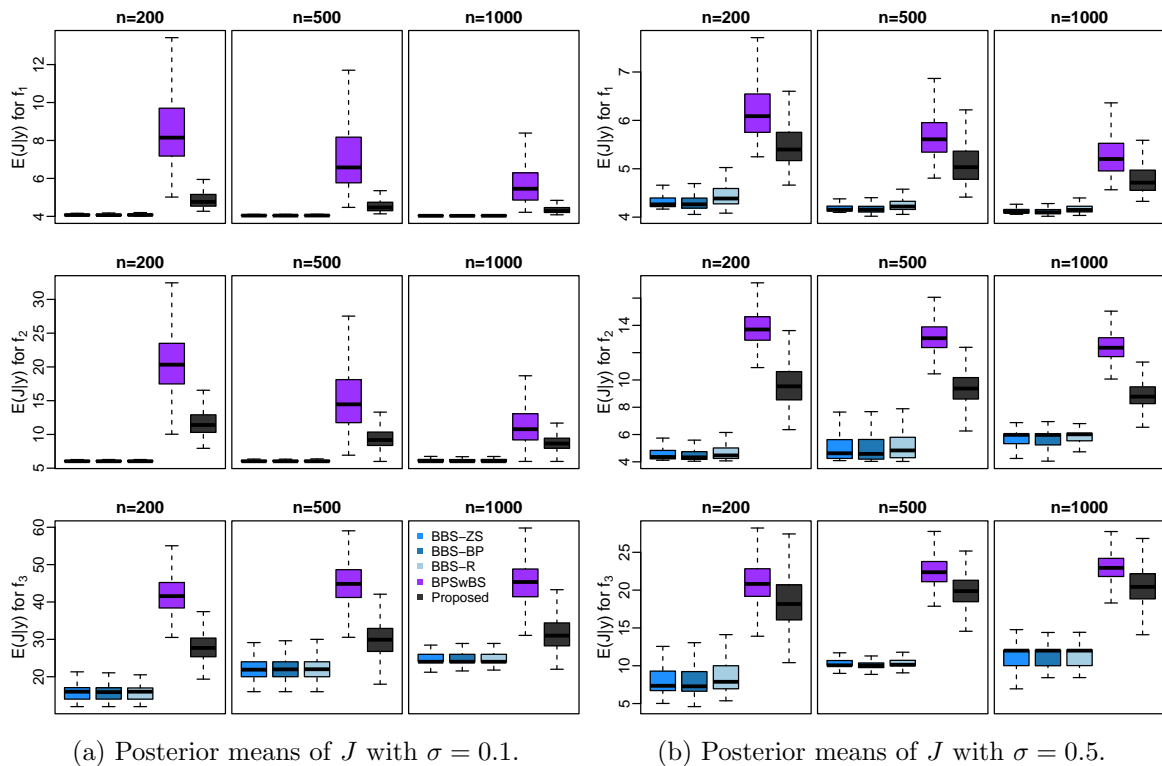


Figure 6: Posterior means of J with the test functions f_1 , f_2 , and f_3 , obtained from 500 replicated datasets.

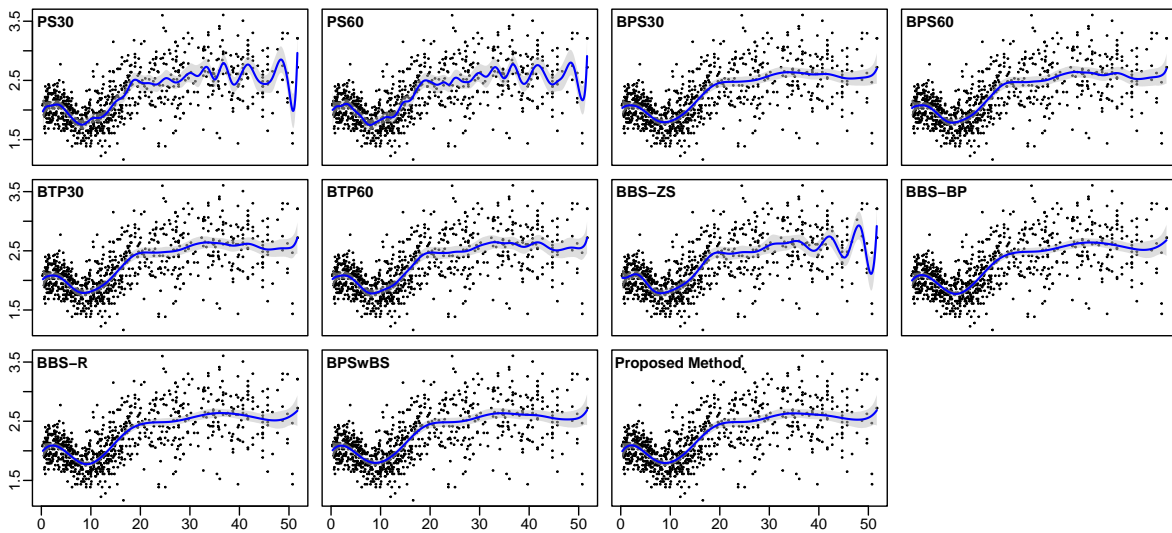


Figure 7: Analysis of the triceps dataset. Each panel visualizes the data points (dots), the estimated function (blue solid line), and the 95% pointwise credible band (grey shaded region).

7 Discussion

In this paper, we propose a new approach to estimate nonparametric regression by integrating penalized regression and basis determination through Bayesian model selection. Although our focus in this paper is on univariate nonparametric regression with a single predictor variable, the framework is readily extendable to incorporate multivariate nonparametric regression models. For example, employing a tensor product of B-splines is useful in modeling multivariate functions. Given that both Bayesian P-splines and Bayesian basis selection are readily applicable to a tensor product of B-splines (Lang and Brezger, 2004; De Jonge and Van Zanten, 2012; Yoo and Ghosal, 2016), our proposed method straightforwardly adapts to such scenarios. Another application is in additive models, where the regression function is parameterized as the sum of univariate functions. The proposed method easily facilitates estimation of each univariate function in an additive model.

Exploring alternative directions for generalization, one might contemplate the use of different basis functions in lieu of B-splines. Natural cubic splines, for instance, can be adopted to mitigate the erratic behaviors often associated with function estimation using B-spline basis functions. Our proposed method is flexible and can be adapted to accommodate various other basis functions as well.

Acknowledgment

The research was supported by the National Research Foundation of Korea (NRF) grant funded by the Korea government (MSIT) (NRF-2022R1C1C1006735, RS-2023-00217705).

A Appendices

This appendix provides the mathematical proofs for the technical results and details of the MCMC algorithm. We first establish the additional notation. For a vector $\mathbf{v} \in \mathbb{R}^m$, $\|\mathbf{v}\|_p$ denotes its ℓ_p -norm. The notations $\rho_{\min}(\cdot)$ and $\rho_{\max}(\cdot)$ are used to denote the minimum and maximum eigenvalues of a square matrix, respectively. For a positive definite matrix, we often write $\rho_{\max}(\cdot) = \|\cdot\|_{\text{sp}}$ using the spectral norm.

A Details of the MCMC Algorithm

A.1 Details of the Slice Sampling

Observe that the target distribution is $\pi(\lambda|J, \tau, \sigma^2, \tilde{\theta}_1, \tilde{\theta}_J, \mathbf{y}) \propto \pi(\lambda)\pi(\tilde{\theta}_J|J, \sigma^2, \lambda, \tau)$. The Gaussian density $\pi(\tilde{\theta}_J|J, \sigma^2, \lambda, \tau)$ is a function of λ that is proportional to the inverse gamma density with parameters $(J-3)/2$ and $\tilde{\theta}_J^T((1-\tau)\tilde{\mathbf{P}}_J + \tau n^{-1}\tilde{\mathbf{B}}_J^T\tilde{\mathbf{B}}_J)\tilde{\theta}_J/(2\sigma^2)$. For the sake of notational simplicity, let $\tilde{\pi}$ denote the posterior density of λ , and let g denote the inverse gamma density as above. Observe that

$$\tilde{\pi}(\lambda) \propto h(\lambda; c_\lambda)g(\lambda) = g(\lambda) \int_0^{h(\lambda; c_\lambda)} d\gamma.$$

The joint density of λ and the auxiliary variable γ is given by

$$\tilde{\pi}(\lambda, \gamma) \propto g(\lambda)I(0 < \gamma < h(\lambda; c_\lambda)).$$

Since an exponential density is monotone, the conditional density of each variable is

$$\begin{aligned}\tilde{\pi}(\lambda \mid \gamma) &\propto g(\lambda)\mathbb{1}\{0 < \lambda < h^{-1}(\gamma; c_\lambda)\}, \\ \tilde{\pi}(\gamma \mid \lambda) &\propto \mathbb{1}\{0 < \gamma < h(\lambda; c_\lambda)\}.\end{aligned}$$

A.2 Details of the Grid Sampling

We only need to verify (8). Observe that

$$\log \pi(\tilde{\boldsymbol{\theta}}_J \mid J, \sigma^2, \lambda, \tau) = \frac{1}{2} \log \left| (1 - \tau)\tilde{\mathbf{P}}_J + \tau n^{-1}\tilde{\mathbf{B}}_J^T \tilde{\mathbf{B}}_J \right| - \frac{1}{2} \tilde{\boldsymbol{\theta}}_J^T \frac{(1 - \tau)\tilde{\mathbf{P}}_J + \tau n^{-1}\tilde{\mathbf{B}}_J^T \tilde{\mathbf{B}}_J}{\lambda \sigma^2} \tilde{\boldsymbol{\theta}}_J + c_1,$$

where c_1 is a constant independent of τ . The determinant term satisfies

$$\begin{aligned}\log \left| (1 - \tau)\tilde{\mathbf{P}}_J + \tau n^{-1}\tilde{\mathbf{B}}_J^T \tilde{\mathbf{B}}_J \right| &= \log \left| \mathbf{I}_{J-1} + (\tau n^{-1}\tilde{\mathbf{B}}_J^T \tilde{\mathbf{B}}_J)^{-1}(1 - \tau)\tilde{\mathbf{P}}_J \right| + \log \left| \tau n^{-1}\tilde{\mathbf{B}}_J^T \tilde{\mathbf{B}}_J \right| \\ &= \sum_{k=1}^{J-1} \log \left(1 + \frac{n(1 - \tau)}{\tau} \rho_k \left((\tilde{\mathbf{B}}_J^T \tilde{\mathbf{B}}_J)^{-1} \tilde{\mathbf{P}}_J \right) \right) + (J - 1) \log \tau + c_2,\end{aligned}$$

where c_2 is a constant independent of τ .

B Proof of Theorem 1

As discussed in Section 4, we first derive a test function with exponentially small errors on small pieces of the parameter space. The following lemma extends Lemma 8.27 of Ghosal and van der Vaart (2017) to incorporate the case of unknown σ_0^2 . The proof is provided in Appendix C.

Lemma 1. *Let $\mathbb{E}_{\boldsymbol{\mu}, \sigma}$ be the expectation operator under $N_n(\boldsymbol{\mu}, \sigma^2 I_n)$, and define $\mathbb{E}_0 = \mathbb{E}_{\boldsymbol{\mu}_0, \sigma_0}$ for some specified $\boldsymbol{\mu}_0$ and σ_0 . Assume that $c^{-1} \leq \sigma_0 \leq c$ for some constant $c \geq 1$. For every $\epsilon > 0$ and $(\boldsymbol{\mu}_1, \sigma_1)$ with $n^{-1}\|\boldsymbol{\mu}_1 - \boldsymbol{\mu}_0\|_2^2 + |\sigma_1 - \sigma_0|^2 \geq \epsilon^2$, there exists a test ϕ_n such that, for a universal constant $K > 0$,*

$$\mathbb{E}_0 \phi_n \leq e^{-K n \epsilon^2}, \quad \sup_{(\boldsymbol{\mu}, \sigma): n^{-1}\|\boldsymbol{\mu} - \boldsymbol{\mu}_1\|_2^2 + |\sigma - \sigma_1|^2 \leq \epsilon^2/36} \mathbb{E}_{\boldsymbol{\mu}, \sigma} (1 - \phi_n) \leq e^{-K n \epsilon^2}.$$

In Section 4, it is discussed that certain challenges arise when employing an inverse gamma prior for σ in conjunction with a hierarchical Gaussian prior on the coefficients. The following lemma allows us to restrict our attention to a bounded set of σ^2 with a suitably increasing order. The proof for this lemma can be found in Appendix C.

Lemma 2. *Under the conditions for Theorem 1, the marginal posterior of σ^2 satisfies $\mathbb{E}_0 \Pi(\sigma > D_n \mid \mathbf{y}) \rightarrow 0$ for any $D_n \rightarrow \infty$.*

Lastly, we specify the eigenvalue bounds for the prior covariance matrix of the coefficients for the original B-spline basis. (Although we assign a prior distribution for the transformed B-spline basis, our theoretical analysis relies on the original construction for the sake of convenience.) This ensures that the prior places sufficient probability mass around the true values while also ensuring exponentially small tails. The proof is given in Appendix C.

Lemma 3. Let $\Sigma_{\sigma,J,\lambda,\tau}$ be the prior variance of θ_J induced from (7). Under Assumption (A3), we obtain that for any $J \lesssim n^{1/(2\alpha+1)}(\log n)^{2\alpha/(2\alpha+1)}$,

$$\begin{aligned}\rho_{\min}(\Sigma_{\sigma,J,\lambda,\tau}) &\gtrsim \sigma^2 / (\lambda^{-1}(1-\tau) + J^{-1} \max(\kappa^{-2}, \tau/\lambda)), \\ \rho_{\max}(\Sigma_{\sigma,J,\lambda,\tau}) &\lesssim \sigma^2 J \max(\kappa^2, \lambda/\tau).\end{aligned}$$

Now, we present the proof of Theorem 1. In this proof, we extend the prior for τ so that its support is $[0, 1]$ while exhibiting an exponential tail on the right side, that is, $\log \Pi(\tau < 1/a_n) \lesssim -a_n$ for any increasing $a_n \rightarrow \infty$. The prior for τ specified in Section 3.1, which is a uniform prior on $(\delta, 1 - \delta)$ with a small $\delta > 0$, clearly satisfies this requirement.

Proof of Theorem 1. Observe that for any $M_n \rightarrow \infty$,

$$\begin{aligned}\Pi(\|f - f_0\|_n + |\sigma - \sigma_0| > M_n \epsilon_n \mid \mathbf{y}) \\ \leq \Pi(\sigma > n \mid \mathbf{y}) + \Pi(\|f - f_0\|_n + |\sigma - \sigma_0| > M_n \epsilon_n \mid \sigma < n, \mathbf{y}).\end{aligned}$$

The expected value of the first term on the right-hand side goes to zero by Lemma 2. The second term is the posterior probability of the given set with the prior for σ that is renormalized and restricted to $\{\sigma^2 : \sigma > n\}$, that is, $\tilde{\Pi}(\cdot) = \Pi(\cdot \mid \sigma < n)$. We also denote the induced posterior by $\tilde{\Pi}(\cdot \mid \mathbf{y})$, so that the second term of the last expression can be expressed as

$$\tilde{\Pi}(\|f - f_0\|_n + |\sigma - \sigma_0| > M_n \epsilon_n \mid \mathbf{y}).$$

We will verify that the expected value of this expression goes to zero using the well-known theory of posterior contraction (Ghosal et al., 2000; Ghosal and van der Vaart, 2007). For the Kullback-Leibler (KL) divergence $K(p_1, p_2) = \int \log(p_1/p_2)p_1$ and its second order variation $V(p_1, p_2) = \int |\log(p_1/p_2) - K(p_1, p_2)|^2 p_1$, define

$$\mathcal{A}_n = \left\{ (f, \sigma) : \sum_{i=1}^n K(p_{0,i}, p_{f,\sigma,i}) \leq n\epsilon_n^2, \sum_{i=1}^n V(p_{0,i}, p_{f,\sigma,i}) \leq n\epsilon_n^2 \right\},$$

where $p_{0,i}$ and $p_{f,\sigma,i}$ are Gaussian densities of individual y_i with the true parameters (f_0, σ_0) and given (f, σ) , respectively. Let $\mathcal{F} = \bigcup_{J=4}^n \mathcal{F}_J$, where

$$\mathcal{F}_J = \left\{ f(\cdot) = \sum_{j=1}^J \theta_j B_j(\cdot) : \theta_J = (\theta_1, \dots, \theta_J)^T \in \mathbb{R}^J \right\}.$$

Since there exists a local test by Lemma 1, due to Theorem 8.11 of Ghosal and van der Vaart (2017), it suffices to show that there exist $\tilde{\mathcal{F}}_n \subset \mathcal{F}$ and $\Xi_n \subset (0, n)$ such that, for some constant $c > 0$ and some sequence $\bar{\epsilon}_n \leq \epsilon_n$ with $n\bar{\epsilon}_n \rightarrow \infty$,

$$\tilde{\Pi}(\mathcal{A}_n) \geq e^{-cn\bar{\epsilon}_n^2}, \tag{9}$$

$$\log N\left(\frac{\epsilon_n}{36}, \tilde{\mathcal{F}}_n \times \Xi_n, d\right) \leq n\epsilon_n^2, \tag{10}$$

$$\tilde{\Pi}((f, \sigma) \notin \tilde{\mathcal{F}}_n \times \Xi_n) = o(e^{-(c+2)n\bar{\epsilon}_n^2}), \tag{11}$$

where $d^2((f_1, \sigma_1), (f_2, \sigma_2)) = \|f_1 - f_2\|_n^2 + |\sigma_1 - \sigma_2|^2$ for any $f_1, f_2 : \mathbb{R} \rightarrow \mathbb{R}$ and $\sigma_1, \sigma_2 \in (0, \infty)$. (This will verify that the posterior contraction for (f, σ) is ϵ_n with respect to d , but $\sqrt{\|\cdot\|_n^2 + |\cdot|^2}$ and $\|\cdot\|_n + |\cdot|$ have the same order.) Below we will show that the conditions in (9)–(11) are satisfied with $\bar{\epsilon}_n \asymp n^{-\alpha/(2\alpha+1)}(\log n)^{1/(2\alpha+1)}$ and $\epsilon_n \asymp n^{-\alpha/(2\alpha+1)}(\log n)^{1/(2\alpha+1)+1}$.

We first verify (9). By direct calculations,

$$\begin{aligned} \frac{1}{n} \sum_{i=1}^n K(p_{0,i}, p_{f,\sigma,i}) &= \frac{1}{2} \log \left(\frac{\sigma^2}{\sigma_0^2} \right) - \frac{1}{2} \left(1 - \frac{\sigma_0^2}{\sigma^2} \right) + \frac{\|f - f_0\|_n^2}{2\sigma^2}, \\ \frac{1}{n} \sum_{i=1}^n V(p_{0,i}, p_{f,\sigma,i}) &= \frac{1}{2} \left(1 - \frac{\sigma_0^2}{\sigma^2} \right)^2 + \frac{\sigma_0^2 \|f - f_0\|_n^2}{\sigma^2}. \end{aligned}$$

Using the Taylor expansion, it is easy to see that, for any $\bar{\epsilon}_n \rightarrow 0$, there exists a constant $C_1 > 0$ such that

$$\mathcal{A}_n \supset \{(f, \sigma) : \|f - f_0\|_n \leq C_1 \bar{\epsilon}_n, |\sigma - \sigma_0| \leq C_1 \bar{\epsilon}_n\}.$$

Therefore,

$$\begin{aligned} \tilde{\Pi}(\mathcal{A}_n) &\geq \tilde{\Pi}\{(f, \sigma) : \|f - f_0\|_n \leq C_1 \bar{\epsilon}_n, |\sigma^2 - \sigma_0^2| \leq C_1 \bar{\epsilon}_n\} \\ &= \int_{\{\sigma^2 : |\sigma^2 - \sigma_0^2| \leq C_1 \bar{\epsilon}_n\}} \Pi(f \in \mathcal{F} : \|f - f_0\|_n \leq C_1 \bar{\epsilon}_n \mid \sigma) d\tilde{\Pi}(\sigma^2) \\ &\geq \tilde{\Pi}(|\sigma^2 - \sigma_0^2| \leq C_1 \bar{\epsilon}_n) \inf_{\sigma^2 : |\sigma^2 - \sigma_0^2| \leq C_1 \bar{\epsilon}_n} \Pi(f \in \mathcal{F} : \|f - f_0\|_n \leq C_1 \bar{\epsilon}_n \mid \sigma). \end{aligned}$$

Since the density of a proper inverse gamma distribution is bounded away from zero on a compact subset of $(0, \infty)$, we obtain that

$$\log \tilde{\Pi}(|\sigma^2 - \sigma_0^2| \leq C_1 \bar{\epsilon}_n) \geq \log \Pi(|\sigma^2 - \sigma_0^2| \leq C_1 \bar{\epsilon}_n) \gtrsim \log \bar{\epsilon}_n \gtrsim -\log n.$$

By restricting J to $\hat{J}_n \asymp (n/\log n)^{1/(2\alpha+1)}$, we obtain

$$\begin{aligned} &\inf_{\sigma^2 : |\sigma^2 - \sigma_0^2| \leq C_1 \bar{\epsilon}_n} \Pi(f \in \mathcal{F} : \|f - f_0\|_n \leq C_1 \bar{\epsilon}_n \mid \sigma) \\ &\geq \Pi(J = \hat{J}_n) \inf_{\sigma^2 : |\sigma^2 - \sigma_0^2| \leq C_1 \bar{\epsilon}_n} \Pi(f \in \mathcal{F}_J : \|f - f_0\|_\infty \leq C_1 \bar{\epsilon}_n \mid \sigma, J = \hat{J}_n). \end{aligned}$$

Observe that a geometric distribution satisfies $\log \Pi(J = \hat{J}_n) \asymp -\hat{J}_n \gtrsim -n\bar{\epsilon}_n^2$ since $\hat{J}_n \log n \asymp n\bar{\epsilon}_n^2$. Moreover, for $f \in \mathcal{F}_J$ with $J = \hat{J}_n$, classical B-spline theory shows that

$$\|f - f_0\|_\infty \leq \|f - \hat{f}\|_\infty + \|\hat{f} - f_0\|_\infty \lesssim \|f - \hat{f}\|_\infty + \hat{J}_n^{-\alpha} \lesssim \|f - \hat{f}\|_\infty + \bar{\epsilon}_n,$$

since $f_0 \in \mathcal{H}^\alpha([0, 1])$ (De Boor, 1978). Therefore, there exists $C_2 > 0$ such that

$$\begin{aligned} &\Pi(f \in \mathcal{F}_J : \|f - f_0\|_\infty \leq C_1 \bar{\epsilon}_n \mid \sigma, J = \hat{J}_n) \\ &\geq \Pi(\boldsymbol{\theta}_J \in \mathbb{R}^J : \|\boldsymbol{\theta}_J - \hat{\boldsymbol{\theta}}_J\|_\infty \leq C_2 \bar{\epsilon}_n \mid \sigma, J = \hat{J}_n) \\ &\geq \Pi\left(\boldsymbol{\theta}_J \in \mathbb{R}^J : \|\boldsymbol{\Sigma}_{\sigma, J, \lambda, \tau}^{-1/2}(\boldsymbol{\theta}_J - \hat{\boldsymbol{\theta}}_J)\|_2 \leq \frac{C_2 \bar{\epsilon}_n}{\sqrt{J \|\boldsymbol{\Sigma}_{\sigma, J, \lambda, \tau}\|_{\text{sp}}}} \mid \sigma, J = \hat{J}_n\right) \\ &\geq \inf_{\lambda \in [1, 2]} \inf_{\tau \in [1/4, 3/4]} \Pi\left(\boldsymbol{\theta}_J \in \mathbb{R}^J : \|\boldsymbol{\Sigma}_{\sigma, J, \lambda, \tau}^{-1/2}(\boldsymbol{\theta}_J - \hat{\boldsymbol{\theta}}_J)\|_2 \leq \frac{C_2 \bar{\epsilon}_n}{\sqrt{J \|\boldsymbol{\Sigma}_{\sigma, J, \lambda, \tau}\|_{\text{sp}}}} \mid \sigma, \lambda, \tau, J = \hat{J}_n\right), \end{aligned}$$

where the last inequality follows since the priors on λ and τ are independent of n and the prior probabilities of compact subsets are bounded away from zero. Using the calculation in page 216 of (Ghosal and van der Vaart, 2007), we obtain that for any $v > 0$,

$$\begin{aligned} & \Pi\left(\boldsymbol{\theta}_J \in \mathbb{R}^J : \|\boldsymbol{\Sigma}_{\sigma, J, \lambda, \tau}^{-1/2}(\boldsymbol{\theta}_J - \hat{\boldsymbol{\theta}}_J)\|_2 \leq v \mid \sigma, \lambda, \tau, J = \hat{J}_n\right) \\ & \geq 2^{-\hat{J}_n/2} \exp\left(-\|\boldsymbol{\Sigma}_{\sigma, \hat{J}_n, \lambda, \tau}^{-1/2} \hat{\boldsymbol{\theta}}_{\hat{J}_n}\|_2^2\right) \Pi\left(\boldsymbol{\theta}_J \in \mathbb{R}^J : \|\boldsymbol{\Sigma}_{\sigma, J, \lambda, \tau}^{-1/2} \boldsymbol{\theta}_J\|_2 \leq v/\sqrt{2} \mid \sigma, \lambda, \tau, J = \hat{J}_n\right). \end{aligned}$$

Using the fact that $\|\boldsymbol{\Sigma}_{\sigma, J, \lambda, \tau}^{-1/2} \boldsymbol{\theta}_J\|_2$ has a χ^2 -distribution with J degrees of freedom, we obtain

$$\begin{aligned} \Pi\left(\boldsymbol{\theta}_J \in \mathbb{R}^J : \|\boldsymbol{\Sigma}_{\sigma, J, \lambda, \tau}^{-1/2} \boldsymbol{\theta}_J\|_2 \leq v/\sqrt{2} \mid \sigma, \lambda, \tau, J = \hat{J}_n\right) & \geq \frac{2/\hat{J}_n}{2^{\hat{J}_n} \Gamma(\hat{J}_n/2)} v^{\hat{J}_n} e^{-v^2/4} \\ & \geq e^{-C_3(\hat{J}_n \log \hat{J}_n + \hat{J}_n \log(1/v) + v^2)}, \end{aligned}$$

for some $C_3 > 0$. Since Lemma 3 implies that

$$\begin{aligned} \inf_{\lambda \in [1, 2]} \inf_{\tau \in [1/4, 3/4]} \|\boldsymbol{\Sigma}_{\sigma, \hat{J}_n, \lambda, \tau}\|_{\text{sp}} & \geq 1/ \sup_{\lambda \in [1, 2]} \sup_{\tau \in [1/4, 3/4]} \rho_{\max}\left(\boldsymbol{\Sigma}_{\sigma, \hat{J}_n, \lambda, \tau}^{-1}\right) \gtrsim \sigma^2, \\ \sup_{\lambda \in [1, 2]} \sup_{\tau \in [1/4, 3/4]} \|\boldsymbol{\Sigma}_{\sigma, \hat{J}_n, \lambda, \tau}\|_{\text{sp}} & = 1/ \inf_{\lambda \in [1, 2]} \inf_{\tau \in [1/4, 3/4]} \rho_{\min}\left(\boldsymbol{\Sigma}_{\sigma, \hat{J}_n, \lambda, \tau}^{-1}\right) \lesssim \sigma^2 \hat{J}_n, \end{aligned}$$

it follows that $\bar{\epsilon}_n/(\sigma \hat{J}_n) \lesssim \bar{\epsilon}_n/\sqrt{\hat{J}_n \|\boldsymbol{\Sigma}_{\sigma, \hat{J}_n, \lambda, \tau}\|_{\text{sp}}} \lesssim \bar{\epsilon}_n/(\sigma \sqrt{\hat{J}_n}) \lesssim 1/\sigma$. Plugging in this, we obtain that

$$\begin{aligned} & \log \inf_{\lambda \in [1, 2]} \inf_{\tau \in [1/4, 3/4]} \Pi\left(\boldsymbol{\theta}_J \in \mathbb{R}^J : \|\boldsymbol{\Sigma}_{\sigma, J, \lambda, \tau}^{-1/2} \boldsymbol{\theta}_J\|_2 \leq \frac{C_2 \bar{\epsilon}_n}{\sqrt{J \|\boldsymbol{\Sigma}_{\sigma, J, \lambda, \tau}\|_{\text{sp}}}} \mid \sigma, \lambda, \tau, J = \hat{J}_n\right) \\ & \gtrsim -\hat{J}_n \log n - \hat{J}_n \log \hat{J}_n - \hat{J}_n \log \sigma - \sigma^{-2}. \end{aligned}$$

Observe also that

$$\begin{aligned} \sup_{\lambda \in [1, 2]} \sup_{\tau \in [1/4, 3/4]} \|\boldsymbol{\Sigma}_{\sigma, \hat{J}_n, \lambda, \tau}^{-1/2} \hat{\boldsymbol{\theta}}_{\hat{J}_n}\|_2^2 & \leq \sup_{\lambda \in [1, 2]} \sup_{\tau \in [1/4, 3/4]} \|\boldsymbol{\Sigma}_{\sigma, \hat{J}_n, \lambda, \tau}^{-1}\|_{\text{sp}} \|\hat{\boldsymbol{\theta}}_{\hat{J}_n}\|_2^2 \\ & \lesssim \sigma^{-2} \hat{J}_n \|\hat{\boldsymbol{\theta}}_{\hat{J}_n}\|_\infty^2 \\ & \lesssim \sigma^{-2} \hat{J}_n. \end{aligned}$$

Combining the bounds, it follows that

$$\begin{aligned} & \log \inf_{\sigma^2: |\sigma^2 - \sigma_0^2| \leq C_1 \bar{\epsilon}_n} \Pi(f \in \mathcal{F}_J : \|f - f_0\|_\infty \leq C_1 \bar{\epsilon}_n \mid \sigma, J = \hat{J}_n) \\ & \geq \log \inf_{\substack{\sigma^2 \in [\sigma_0^2/2, 2\sigma_0^2], \\ \lambda \in [1, 2], \tau \in [1/4, 3/4]}} \Pi\left(\boldsymbol{\theta}_J \in \mathbb{R}^J : \|\boldsymbol{\Sigma}_{\sigma, J, \lambda, \tau}^{-1/2}(\boldsymbol{\theta}_J - \hat{\boldsymbol{\theta}}_J)\|_2 \leq \frac{C_2 \bar{\epsilon}_n}{\sqrt{J \|\boldsymbol{\Sigma}_{\sigma, J, \lambda, \tau}\|_{\text{sp}}}} \mid \sigma, \lambda, \tau, J = \hat{J}_n\right) \\ & \gtrsim -\hat{J}_n \log n. \end{aligned}$$

Putting everything together, we obtain that $\tilde{\Pi}(\mathcal{A}_n) \geq e^{-cn\bar{\epsilon}_n^2}$ for some $c > 0$.

Next, we verify (10). Let $\Xi_n = (0, n)$ and

$$\tilde{\mathcal{F}}_n = \bigcup_{J \leq \bar{J}_n} \{f \in \mathcal{F}_J : \|\boldsymbol{\theta}_J\|_\infty \leq n^{D_1}\},$$

for a constant $D_1 > 0$, where $\bar{J}_n = \lfloor D_2 \hat{J}_n \log n \rfloor$ for a constant $D_2 > 0$. Since $\|\sum_{j=1}^J \theta_j B_j(\cdot)\|_n \leq \|\sum_{j=1}^J \theta_j B_j(\cdot)\|_\infty \leq \|\boldsymbol{\theta}_J\|_\infty$ by Lemma E.6 of Ghosal and van der Vaart (2017), it follows that

$$\begin{aligned} \log N\left(\frac{\epsilon_n}{36}, \tilde{\mathcal{F}}_n \times \Xi_n, d\right) &\leq \log N\left(\frac{\epsilon_n}{36}, \tilde{\mathcal{F}}_n, \|\cdot\|_n\right) + \log N\left(\frac{\epsilon_n}{36}, \Xi_n, |\cdot|\right) \\ &\leq \log \left\{ \sum_{J \leq \bar{J}_n} N\left(\frac{\epsilon_n}{36}, \{\boldsymbol{\theta}_J \in \mathbb{R}^J : \|\boldsymbol{\theta}_J\|_\infty \leq n^{D_1}\}, \|\cdot\|_\infty\right) \right\} + \log(18n/\epsilon_n) \\ &\leq \log(\bar{J}_n (108n^{D_1}/\epsilon_n)^{\bar{J}_n}) + \log(18n/\epsilon_n). \end{aligned}$$

Since the rightmost side is bounded by a multiple of $\bar{J}_n \log n$, it is bounded by $n\epsilon_n^2$ by choosing $\epsilon_n = D_3 n^{-\alpha/(2\alpha+1)} (\log n)^{1/(2\alpha+1)+1}$ for a sufficiently large $D_3 > 0$, regardless of how large D_1 and D_2 are.

To verify (11), observe that

$$\begin{aligned} \tilde{\Pi}((f, \sigma) \notin \tilde{\mathcal{F}}_n \times \Xi_n) &\leq \Pi(J > \bar{J}_n) + \Pi(\lambda > n) + \Pi(\tau < 1/n) \\ &\quad + \tilde{\Pi}(\|\boldsymbol{\theta}_J\|_\infty > n^{D_1}, J \leq \bar{J}_n, \lambda \leq n, \tau \geq 1/n). \end{aligned}$$

Observe that $\log \Pi(J > \bar{J}_n) \asymp -\bar{J}_n$, $\log \Pi(\lambda > n) \asymp -n$, and $\log \Pi(\tau < 1/n) \lesssim -n$. If D_2 is chosen to be sufficiently large, it follows that $\Pi(J > \bar{J}_n) + \Pi(\lambda > n) + \Pi(\tau < 1/n) = o(e^{-(c+2)n\epsilon_n^2})$. Moreover,

$$\begin{aligned} &\tilde{\Pi}(\|\boldsymbol{\theta}_J\|_\infty > n^{D_1}, J \leq \bar{J}_n, \lambda \leq n, \tau \geq 1/n) \\ &= \sum_{j=q+1}^{\bar{J}_n} \Pi(J = j) \int_{1/n}^1 \int_0^n \int_0^n \Pi(\|\boldsymbol{\theta}_J\|_\infty > n^{D_1} \mid \sigma^2, \lambda, \tau, J = j) d\tilde{\Pi}(\sigma^2) d\Pi(\lambda) d\Pi(\tau) \\ &\leq \max_{j \leq \bar{J}_n} \sup_{\sigma^2 \in (0, n)} \sup_{\lambda \in (0, n)} \sup_{\tau \in (1/n, 1)} \Pi(\|\boldsymbol{\theta}_J\|_\infty > n^{D_1} \mid \sigma^2, \lambda, \tau, J = j) \\ &\leq \max_{j \leq \bar{J}_n} \sup_{\sigma^2 \in (0, n)} \sup_{\lambda \in (0, n)} \sup_{\tau \in (1/n, 1)} \Pi\left(\|\boldsymbol{\Sigma}_{\sigma, J, \lambda, \tau}^{-1/2} \boldsymbol{\theta}_J\|_\infty > n^{D_1} / \sqrt{J \|\boldsymbol{\Sigma}_{\sigma, J, \lambda, \tau}\|_{\text{sp}}} \mid \sigma^2, \lambda, \tau, J = j\right) \\ &\leq \sup_{\sigma^2 \in (0, n)} \sup_{\lambda \in (0, n)} \sup_{\tau \in (1/n, 1)} 2\bar{J}_n \exp\left(-\frac{n^{2D_1}}{2\bar{J}_n \|\boldsymbol{\Sigma}_{\sigma, \bar{J}_n, \lambda, \tau}\|_{\text{sp}}}\right). \end{aligned}$$

Since $\bar{J}_n \leq n$ and $\|\boldsymbol{\Sigma}_{\sigma, \bar{J}_n, \lambda, \tau}\|_{\text{sp}} = 1/\rho_{\min}(\boldsymbol{\Sigma}_{\sigma, \bar{J}_n, \lambda, \tau}^{-1}) \leq \sigma^2 \bar{J}_n \max\{\kappa^2, \lambda/\tau\}$, the rightmost side of the last expression is bounded by e^{-n} as long as D_1 is suitably chosen, and hence is $o(e^{-(c+2)n\epsilon_n^2})$. \square

C Proofs of the Remaining Technical Results

Proof of Proposition 1. We will find a linear bijection $\mathbf{A}_J : \boldsymbol{\theta}_J \mapsto \tilde{\boldsymbol{\theta}}_J^* = (\tilde{\theta}_1, \tilde{\boldsymbol{\theta}}_J^T)^T$ such that $\sum_{j=1}^J \theta_j B_j(\cdot) = \tilde{\theta}_1 + \sum_{j=2}^J \tilde{\theta}_j \tilde{B}_j(\cdot)$. Using the sum-to-unity property of B-splines, observe that

$$\begin{aligned} \sum_{j=1}^J \theta_j B_j(\cdot) &= \theta_1 \left(1 - \sum_{j=2}^J B_j(\cdot) \right) + \sum_{j=2}^J \theta_j B_j(\cdot) \\ &= \theta_1 + \sum_{j=2}^J (\theta_j - \theta_1) c_j + \sum_{j=2}^J (\theta_j - \theta_1) (B_j(\cdot) - c_j) \\ &= \sum_{j=1}^J \theta_j c_j + \sum_{j=2}^J (\theta_j - \theta_1) \tilde{B}_j(\cdot), \end{aligned}$$

where $c_j = n^{-1} \sum_{i=1}^n B_j(x_i)$. Letting $\tilde{\theta}_1 = \sum_{j=1}^J c_j \theta_j$ and $\tilde{\theta}_j = -\theta_1 + \theta_j$ for $j = 2, \dots, J$, we obtain

$$\mathbf{A}_J = \begin{pmatrix} c_1 & c_2 & c_3 & \dots & c_{J-1} & c_J \\ -1 & 1 & 0 & \dots & 0 & 0 \\ -1 & 0 & 1 & \dots & 0 & 0 \\ \vdots & \vdots & \vdots & \ddots & \vdots & \vdots \\ -1 & 0 & 0 & \dots & 1 & 0 \\ -1 & 0 & 0 & \dots & 0 & 1 \end{pmatrix} \in \mathbb{R}^{J \times J}. \quad (12)$$

Observe that $(\mathbf{0}, \tilde{\mathbf{D}}_J) \mathbf{A}_J = \mathbf{D}_J$. Therefore, $\boldsymbol{\theta}_J^T \mathbf{P}_J \boldsymbol{\theta}_J = (\mathbf{D}_J \mathbf{A}_J^{-1} \tilde{\boldsymbol{\theta}}_J^*)^T \mathbf{D}_J \mathbf{A}_J^{-1} \tilde{\boldsymbol{\theta}}_J^* = \tilde{\boldsymbol{\theta}}_J^T \tilde{\mathbf{P}}_J \tilde{\boldsymbol{\theta}}_J$. It is also obvious that $\text{rank}(\mathbf{P}_J) = \text{rank}(\tilde{\mathbf{P}}_J)$. This verifies the assertion. \square

Proof of Lemma 1. We write $\mathbf{y} \sim N_n(\boldsymbol{\mu}, \sigma^2 I_n)$. Let $P_{\boldsymbol{\mu}, \sigma}$ be the probability measure of $N_n(\boldsymbol{\mu}, \sigma^2 I_n)$, and define $P_0 = P_{\boldsymbol{\mu}_0, \sigma_0}$ for $\boldsymbol{\mu}_0$ and σ_0 . We separate the range of the parameters as follows.

- *Case 1:* $\sigma > M_1 \sigma_0$.
- *Case 2:* $\sigma \leq M_1 \sigma_0$ and $7 \|\boldsymbol{\mu}_1 - \boldsymbol{\mu}_0\|_2^2 > n |\sigma_1 - \sigma_0|^2$.
- *Case 3:* $\sigma \leq M_1 \sigma_0$, $\sigma_0 \leq \sigma_1$ and $7 \|\boldsymbol{\mu}_1 - \boldsymbol{\mu}_0\|_2^2 \leq n |\sigma_1 - \sigma_0|^2$.
- *Case 4:* $\sigma \leq M_1 \sigma_0$, $\sigma_0 > \sigma_1$ and $7 \|\boldsymbol{\mu}_1 - \boldsymbol{\mu}_0\|_2^2 \leq n |\sigma_1 - \sigma_0|^2$.

Case 1: Define the test function $\phi_{1,n} = \mathbb{1}\{\|\mathbf{y} - \boldsymbol{\mu}_0\|_2^2 > M_0 n \epsilon^2\}$. Under the measure P_0 , $\|\mathbf{y} - \boldsymbol{\mu}_0\|_2^2 / \sigma_0^2$ has a chi-squared distribution with n degrees of freedom. Hence using the tail bound of chi-squared distributions (Laurent and Massart, 2000, Lemma 1), we obtain that $\mathbb{E}_0 \phi_{1,n} \leq e^{-K_1 n \epsilon^2}$ for some $K_1 > 0$ since σ_0 is bounded, as soon as M_0 is suitably large. Observe also that under $P_{\boldsymbol{\mu}, \sigma}$, $\|\mathbf{y} - \boldsymbol{\mu}_0\|_2^2 / \sigma^2$ has a noncentral chi-squared distribution with n degrees of freedom and noncentrality parameter $\|\boldsymbol{\mu} - \boldsymbol{\mu}_0\|_2^2 / \sigma^2$. Let $W_{k, \gamma}$ be a chi-squared random variable with k degrees of freedom and noncentrality parameter γ . We then obtain

$$\mathbb{E}_{\boldsymbol{\mu}, \sigma} (1 - \phi_{1,n}) = P_{\boldsymbol{\mu}, \sigma} \left\{ \frac{\|\mathbf{y} - \boldsymbol{\mu}_0\|_2^2}{\sigma^2} \leq \frac{M_0 n \epsilon^2}{\sigma^2} \right\} \leq \Pr \left\{ W_{n,0} \leq \frac{M_0 n \epsilon^2}{M_1^2 \sigma_0^2} \right\},$$

using the fact that $\Pr(W_{n,a} \leq \xi) \leq \Pr(W_{n,b} \leq \xi)$ for every $a \geq b$. Since σ_0 is bounded, choosing a suitably large M_1 , the tail bound of chi-squared distributions gives an upper bound $e^{-K_2 n \epsilon^2}$ of the expression for some $K_2 > 0$.

Case 2: Define the test $\phi_{2,n} = \mathbb{1}\{(\boldsymbol{\mu}_1 - \boldsymbol{\mu}_0)^T(\mathbf{y} - \boldsymbol{\mu}_0) > \|\boldsymbol{\mu}_1 - \boldsymbol{\mu}_0\|_2^2/2\}$. Since $8n^{-1}\|\boldsymbol{\mu}_1 - \boldsymbol{\mu}_0\|_2^2 \geq n^{-1}\|\boldsymbol{\mu}_1 - \boldsymbol{\mu}_0\|_2^2 + |\sigma_1 - \sigma_0|^2 \geq \epsilon^2$ and σ_0 is bounded above, we easily obtain $\mathbb{E}_0 \phi_{2,n} = \Phi(-\|\boldsymbol{\mu}_1 - \boldsymbol{\mu}_0\|_2/(2\sigma_0)) \leq e^{-K_3 n \epsilon^2}$ for some $K_3 > 0$, using the Gaussian concentration inequality. For the error probability of the second kind, observe that $2(\boldsymbol{\mu}_1 - \boldsymbol{\mu}_0)^T(\boldsymbol{\mu} - \boldsymbol{\mu}_0) = \|\boldsymbol{\mu}_1 - \boldsymbol{\mu}_0\|_2^2 + \|\boldsymbol{\mu} - \boldsymbol{\mu}_0\|_2^2 - \|\boldsymbol{\mu} - \boldsymbol{\mu}_1\|_2^2$ and $\|\boldsymbol{\mu} - \boldsymbol{\mu}_0\|_2^2 \geq \|\boldsymbol{\mu}_1 - \boldsymbol{\mu}_0\|_2^2/2 - \|\boldsymbol{\mu} - \boldsymbol{\mu}_1\|_2^2$. It follows that

$$\begin{aligned} \mathbb{E}_{\boldsymbol{\mu},\sigma}(1 - \phi_{2,n}) &= P_{\boldsymbol{\mu},\sigma} \left\{ (\boldsymbol{\mu}_1 - \boldsymbol{\mu}_0)^T(\mathbf{y} - \boldsymbol{\mu}) \leq \|\boldsymbol{\mu} - \boldsymbol{\mu}_1\|_2^2/2 - \|\boldsymbol{\mu} - \boldsymbol{\mu}_0\|_2^2/2 \right\} \\ &\leq P_{\boldsymbol{\mu},\sigma} \left\{ \frac{(\boldsymbol{\mu}_1 - \boldsymbol{\mu}_0)^T(\mathbf{y} - \boldsymbol{\mu})}{\sigma \|\boldsymbol{\mu}_1 - \boldsymbol{\mu}_0\|_2} \leq \frac{\|\boldsymbol{\mu} - \boldsymbol{\mu}_1\|_2^2}{\sigma \|\boldsymbol{\mu}_1 - \boldsymbol{\mu}_0\|_2} - \frac{\|\boldsymbol{\mu}_1 - \boldsymbol{\mu}_0\|_2}{4\sigma} \right\}. \end{aligned}$$

Since $\|\boldsymbol{\mu}_1 - \boldsymbol{\mu}_0\|_2^2 \geq n\epsilon^2/8$ and $\|\boldsymbol{\mu} - \boldsymbol{\mu}_1\|_2^2 \leq n\epsilon^2/36$, the rightmost side is bounded by $\Phi(-\sqrt{n}\epsilon/(72\sqrt{2}\sigma)) \leq \Phi(-\sqrt{n}\epsilon/(72\sqrt{2}M_1\sigma_0)) \leq e^{-K_4 n \epsilon^2}$ for some $K_4 > 0$.

Case 3: Define the test $\phi_{3,n} = \mathbb{1}\{n^{-1}\|\mathbf{y} - \boldsymbol{\mu}_0\|_1 - \sqrt{2/\pi}\sigma_0 > \sqrt{2/\pi}(\sigma_1 - \sigma_0)/12\}$. Let $\mathbf{z} \sim N_n(\mathbf{0}_n, \mathbf{I}_n)$ and observe that $\mathbb{E}\|\mathbf{z}\|_1 = n\sqrt{2/\pi}$. Then,

$$\mathbb{E}_0 \phi_{3,n} = \Pr \left\{ \|\mathbf{z}\|_1 - \mathbb{E}\|\mathbf{z}\|_1 > \frac{\sqrt{2/\pi}n}{12\sigma_0}(\sigma_1 - \sigma_0) \right\} \leq \Pr \left\{ \|\mathbf{z}\|_1 - \mathbb{E}\|\mathbf{z}\|_1 > \frac{\sqrt{7}n\epsilon}{24\sqrt{\pi}\sigma_0} \right\}, \quad (13)$$

since $\sigma_0 \leq \sigma_1$ and $(1 + 1/7)|\sigma_1 - \sigma_0|^2 \geq n^{-1}\|\boldsymbol{\mu}_1 - \boldsymbol{\mu}_0\|_2^2 + |\sigma_1 - \sigma_0|^2 \geq \epsilon^2$. Note that $\|\mathbf{z}\|_1 - \mathbb{E}\|\mathbf{z}\|_1$ is the sum of independent sub-Gaussian random variables with mean zero. It thus satisfies the concentration inequality of the form $P(|\|\mathbf{z}\|_1 - \mathbb{E}\|\mathbf{z}\|_1| > \xi) \leq e^{-K'\xi^2/n}$ for some $K' > 0$, (Wainwright, 2019, Proposition 2.5). This gives an upper bound $e^{-K_5 n \epsilon^2}$ of (13) for some $K_5 > 0$. Observe also that

$$\begin{aligned} \mathbb{E}_{\boldsymbol{\mu},\sigma}(1 - \phi_{3,n}) &\leq P_{\boldsymbol{\mu},\sigma} \left\{ n^{-1}\|\mathbf{y} - \boldsymbol{\mu}\|_1 - \sqrt{2/\pi}\sigma_0 \leq \frac{\sqrt{2/\pi}}{12}(\sigma_1 - \sigma_0) + n^{-1/2}\|\boldsymbol{\mu} - \boldsymbol{\mu}_0\|_2 \right\} \\ &= \Pr \left\{ \|\mathbf{z}\|_1 - \mathbb{E}\|\mathbf{z}\|_1 \leq \frac{n}{\sigma} \left[\frac{\sqrt{2/\pi}}{12}(\sigma_1 - \sigma_0) + \sqrt{2/\pi}(\sigma_0 - \sigma) + n^{-1/2}\|\boldsymbol{\mu} - \boldsymbol{\mu}_0\|_2 \right] \right\}. \end{aligned}$$

The term in the bracket is bounded by

$$\begin{aligned} &-\frac{11}{12}\sqrt{2/\pi}(\sigma_1 - \sigma_0) + \sqrt{2/\pi}(\sigma_1 - \sigma) + n^{-1/2}\|\boldsymbol{\mu}_1 - \boldsymbol{\mu}_0\|_2 + n^{-1/2}\|\boldsymbol{\mu} - \boldsymbol{\mu}_1\|_2 \\ &\leq \left(-\frac{11}{12}\sqrt{2/\pi} + \frac{1}{\sqrt{7}} \right) (\sigma_1 - \sigma_0) + n^{-1/2}\|\boldsymbol{\mu} - \boldsymbol{\mu}_1\|_2 + |\sigma - \sigma_1| \\ &\leq -\frac{7}{20}(\sigma_1 - \sigma_0) + \sqrt{2(n^{-1}\|\boldsymbol{\mu} - \boldsymbol{\mu}_1\|_2^2 + |\sigma - \sigma_1|^2)}. \end{aligned} \quad (14)$$

Using the fact that $(1 + 1/7)|\sigma_1 - \sigma_0|^2 \geq \epsilon^2$, we can further bound the rightmost side by $[-(7/20)\sqrt{7/8} + \sqrt{2}/6]\epsilon < -\epsilon/11$. Therefore, $\mathbb{E}_{\boldsymbol{\mu},\sigma}(1 - \phi_{3,n}) \leq P(\|\mathbf{z}\|_1 - \mathbb{E}\|\mathbf{z}\|_1 \leq -n\epsilon/(11M_1\sigma_0)) \leq e^{-K_6 n \epsilon^2}$ for some $K_6 > 0$.

Case 4: Define the test function $\phi_{4,n} = \mathbb{1}\{n^{-1}\|\mathbf{y} - \boldsymbol{\mu}_0\|_1 - \sigma_0\sqrt{2/\pi} \leq \sqrt{2/\pi}(\sigma_1 - \sigma_0)/12\}$. Since $\sigma_0 > \sigma_1$ and $(1+1/7)|\sigma_1 - \sigma_0|^2 \geq \epsilon^2$, we obtain $\mathbb{E}_0\phi_{4,n} \leq \Pr\{\|\mathbf{z}\|_1 - \mathbb{E}\|\mathbf{z}\|_1 \leq -\sqrt{7}n\epsilon/(24\sqrt{\pi}\sigma_0)\} \leq e^{-K_7n\epsilon^2}$ for some $K_7 > 0$, similar to the case with $\phi_{3,n}$. Also observe that

$$\begin{aligned} & \mathbb{E}_{\boldsymbol{\mu},\sigma}(1 - \phi_{4,n}) \\ & \leq \Pr\left\{\|\mathbf{z}\|_1 - \mathbb{E}\|\mathbf{z}\|_1 > \frac{n}{\sigma}\left[\frac{-\sqrt{2/\pi}}{12}(\sigma_0 - \sigma_1) + \sqrt{2/\pi}(\sigma_0 - \sigma) - n^{-1/2}\|\boldsymbol{\mu} - \boldsymbol{\mu}_0\|_2\right]\right\}. \end{aligned}$$

Using the inequality in (14), the term in the bracket is bounded below by

$$\begin{aligned} & \frac{11}{12}\sqrt{2/\pi}(\sigma_0 - \sigma_1) + \sqrt{2/\pi}(\sigma_1 - \sigma) - n^{-1/2}\|\boldsymbol{\mu}_1 - \boldsymbol{\mu}_0\|_2 - n^{-1/2}\|\boldsymbol{\mu} - \boldsymbol{\mu}_1\|_2 \\ & \geq \frac{7}{20}(\sigma_1 - \sigma_0) - \sqrt{2(n^{-1}\|\boldsymbol{\mu} - \boldsymbol{\mu}_1\|_n^2 + |\sigma - \sigma_1|^2)} \\ & \geq \epsilon/11. \end{aligned}$$

Hence, $\mathbb{E}_{\boldsymbol{\mu},\sigma}(1 - \phi_{4,n}) \leq \Pr\{\|\mathbf{z}\|_1 - \mathbb{E}\|\mathbf{z}\|_1 > n\epsilon/(11M_1\sigma_0)\} \leq e^{-K_8n\epsilon^2}$ for some $K_8 > 0$.

We can construct the test function ϕ_n by combining *Case 1* to *Case 4* to obtain the union bound as in the lemma. \square

Proof of Lemma 2. By Markov's inequality,

$$\mathbb{E}_0\Pi(\sigma > D_n \mid \mathbf{y}) \leq D_n^{-2}\mathbb{E}_0\mathbb{E}(\sigma^2 \mid \mathbf{y}).$$

By Fubini's theorem,

$$\begin{aligned} \mathbb{E}_0\mathbb{E}(\sigma^2 \mid \mathbf{y}) &= \int \int \mathbb{E}(\sigma^2 \mid J, \lambda, \tau, \mathbf{y}) d\Pi(J, \lambda, \tau \mid \mathbf{y}) dP_0 \\ &= \int \mathbb{E}_0\mathbb{E}(\sigma^2 \mid J, \lambda, \tau, \mathbf{y}) d\Pi(J, \lambda, \tau \mid \mathbf{y}) \\ &\leq \sup_{J \leq n, \lambda > 0, \tau \in [0,1]} \mathbb{E}_0\mathbb{E}(\sigma^2 \mid J, \lambda, \tau, \mathbf{y}). \end{aligned}$$

If $a_\sigma + n/2 > 1$, we obtain that

$$\mathbb{E}(\sigma^2 \mid J, \lambda, \tau, \mathbf{y}) = \frac{2b_\sigma + n\hat{\sigma}_{J,\lambda,\tau}^2}{2a_\sigma + n - 2} \asymp \hat{\sigma}_{J,\lambda,\tau}^2,$$

where

$$\hat{\sigma}_{J,\lambda,\tau}^2 = \frac{1}{n} \left[\mathbf{y}^T \mathbf{y} - \frac{(\mathbf{y}^T \mathbf{1}_n)^2}{n + \kappa^2} - \mathbf{y}^T \tilde{\mathbf{B}}_J \boldsymbol{\Omega}_{J,\lambda,\tau}^{-1} \tilde{\mathbf{B}}_J^T \mathbf{y} \right] = \frac{1}{n} \mathbf{y}^T \left[\mathbf{I}_n - \frac{\mathbf{1}_n \mathbf{1}_n^T}{n + \kappa^2} - \tilde{\mathbf{B}}_J \boldsymbol{\Omega}_{J,\lambda,\tau}^{-1} \tilde{\mathbf{B}}_J^T \right] \mathbf{y}.$$

Let $\mathbf{U}_{J,\lambda,\tau} = \mathbf{I}_n - (\mathbf{1}_n \mathbf{1}_n^T)/(n + \kappa^2) - \tilde{\mathbf{B}}_J \boldsymbol{\Omega}_{J,\lambda,\tau}^{-1} \tilde{\mathbf{B}}_J^T$. Since $\mathbb{E}_0(\mathbf{y}^T \mathbf{A} \mathbf{y}) = \sigma_0^2 \text{tr}(\mathbf{A}) + \mathbb{E}_0(\mathbf{y})^T \mathbf{A} \mathbb{E}_0(\mathbf{y})$ for a symmetric matrix \mathbf{A} ,

$$\begin{aligned} |\mathbb{E}_0(\hat{\sigma}_{J,\lambda,\tau}^2) - \sigma_0^2| &\leq |n^{-1}\sigma_0^2 \text{tr}(\mathbf{U}_{J,\lambda,\tau}) - \sigma_0^2| + n^{-1} \mathbf{f}_0^T \mathbf{U}_{J,\lambda,\tau} \mathbf{f}_0 \\ &\leq n^{-1}\sigma_0^2 \text{tr}(\mathbf{I}_n - \mathbf{U}_{J,\lambda,\tau}) + n^{-1} \|\mathbf{U}_{J,\lambda,\tau}\|_{\text{sp}} \|\mathbf{f}_0\|_2^2, \end{aligned} \tag{15}$$

where $\mathbf{f}_0 = \mathbb{E}_0(\mathbf{y})$. Observe that

$$\begin{aligned}\mathrm{tr}(\mathbf{I}_n - \mathbf{U}_{J,\lambda,\tau}) &= \frac{n}{n + \kappa^2} + \mathrm{tr}\left(\tilde{\mathbf{B}}_J \boldsymbol{\Omega}_{J,\lambda,\tau}^{-1} \tilde{\mathbf{B}}_J^T\right) \\ &= \frac{n}{n + \kappa^2} + \left(1 + \frac{\tau}{\lambda n}\right)^{-1} \mathrm{tr}\left(\boldsymbol{\Omega}_{J,\lambda,\tau}^{-1} \left(1 + \frac{\tau}{\lambda n}\right) \tilde{\mathbf{B}}_J^T \tilde{\mathbf{B}}_J\right) \\ &\leq 1 + (J - 1) = J,\end{aligned}$$

where the inequality holds since

$$\begin{aligned}\mathrm{tr}\left(\boldsymbol{\Omega}_{J,\lambda,\tau}^{-1} \left(1 + \frac{\tau}{\lambda n}\right) \tilde{\mathbf{B}}_J^T \tilde{\mathbf{B}}_J\right) &= \mathrm{tr}\left(\mathbf{I}_{J-1} - \boldsymbol{\Omega}_{J,\lambda,\tau}^{-1} \left(\frac{1-\tau}{\lambda}\right) \tilde{\mathbf{P}}_J\right) \\ &= (J - 1) - \left(\frac{1-\tau}{\lambda}\right) \mathrm{tr}\left(\tilde{\mathbf{D}}_J \boldsymbol{\Omega}_{J,\lambda,\tau}^{-1} \tilde{\mathbf{D}}_J^T\right) \\ &\leq J - 1,\end{aligned}$$

due to the positive semi-definiteness of $\tilde{\mathbf{D}}_J \boldsymbol{\Omega}_{J,\lambda,\tau}^{-1} \tilde{\mathbf{D}}_J^T$. It is also easy to see that $\|\mathbf{U}_{J,\lambda,\tau}\|_{\mathrm{sp}} \leq 1$ because $(\mathbf{1}_n \mathbf{1}_n^T)/(n + \kappa^2) + \tilde{\mathbf{B}}_J \boldsymbol{\Omega}_{J,\lambda,\tau}^{-1} \tilde{\mathbf{B}}_J^T$ is positive semi-definite. Hence, (15) is bounded by a constant multiple of $J/n + 1$ under (A1) and (A2). This implies that $\mathbb{E}_0 \mathbb{E}(\sigma^2 \mid \mathbf{y})$ is bounded, and the assertion follows as soon as D_n is increasing. \square

Proof of Lemma 3. Observe that $\boldsymbol{\theta}_J^* = \mathbf{A}_J \boldsymbol{\theta}_J$ with \mathbf{A}_J in (12). Thus, we obtain that

$$\begin{aligned}\boldsymbol{\Sigma}_{\sigma,J,\lambda,\tau}^{-1} &= \sigma^{-2} \mathbf{A}_J^T \begin{pmatrix} \kappa^{-2} & \mathbf{0}^T \\ \mathbf{0} & \lambda^{-1} \left((1-\tau) \tilde{\mathbf{P}}_J + \tau n^{-1} \tilde{\mathbf{B}}_J^T \tilde{\mathbf{B}}_J \right) \end{pmatrix} \mathbf{A}_J \\ &= \sigma^{-2} \left\{ \lambda^{-1} (1-\tau) \mathbf{A}_J^T \begin{pmatrix} 0 & \mathbf{0}^T \\ \mathbf{0} & \tilde{\mathbf{P}}_J \end{pmatrix} \mathbf{A}_J + \mathbf{A}_J^T \begin{pmatrix} \kappa^{-2} & \mathbf{0}^T \\ \mathbf{0} & \tau/(\lambda n) \tilde{\mathbf{B}}_J^T \tilde{\mathbf{B}}_J \end{pmatrix} \mathbf{A}_J \right\}.\end{aligned}\tag{16}$$

Since $(\mathbf{0}, \tilde{\mathbf{D}}_J) \mathbf{A}_J = \mathbf{D}_J$, (16) is equal to

$$\sigma^{-2} \left\{ \lambda^{-1} (1-\tau) \mathbf{P}_J + \mathbf{A}_J^T \mathbf{R}_J^T \mathbf{R}_J \mathbf{A}_J \right\},$$

where

$$\mathbf{R}_J = \begin{pmatrix} \mathbf{1}_n & \tilde{\mathbf{B}}_J \\ \mathbf{0} & \sqrt{\tau/(\lambda n)} \mathbf{I}_{J-1} \end{pmatrix}.$$

Therefore, since $(\mathbf{1}_n, \tilde{\mathbf{B}}_J) \mathbf{A}_J = \mathbf{B}_J$, we obtain that

$$\begin{aligned}\rho_{\min}(\boldsymbol{\Sigma}_{\sigma,J,\lambda,\tau}^{-1}) &\geq \sigma^{-2} \left\{ \lambda^{-1} (1-\tau) \rho_{\min}(\mathbf{P}_J) + n^{-1} \min(\kappa^{-2}, \tau/\lambda) \rho_{\min}(\mathbf{B}_J^T \mathbf{B}_J) \right\}, \\ \rho_{\max}(\boldsymbol{\Sigma}_{\sigma,J,\lambda,\tau}^{-1}) &\leq \sigma^{-2} \left\{ \lambda^{-1} (1-\tau) \rho_{\max}(\mathbf{P}_J) + n^{-1} \max(\kappa^{-2}, \tau/\lambda) \rho_{\max}(\mathbf{B}_J^T \mathbf{B}_J) \right\}.\end{aligned}$$

According to Lemma 6.2 of Shen et al. (1998) or Lemma A.9 of Yoo and Ghosal (2016), we can conclude that $n/J \lesssim \rho_{\min}(\mathbf{B}_J^T \mathbf{B}_J) \leq \rho_{\max}(\mathbf{B}_J^T \mathbf{B}_J) \lesssim n/J$ for any $J \lesssim n^{1/(2\alpha+1)} (\log n)^{2\alpha/(2\alpha+1)}$ under Assumption (A3). It is clear that $\rho_{\min}(\mathbf{P}_J) = 0$. To find an upper bound for $\rho_{\max}(\mathbf{P}_J)$, observe that $\mathbf{P}_J = \mathbf{D}_J^T \mathbf{D}_J$ and $\mathbf{D}_J \mathbf{D}_J^T$ share the identical nonzero eigenvalues. Since the latter is a symmetric banded Toeplitz matrix, Lemma 6 of Gray et al. (2006) shows that $\rho_{\max}(\mathbf{P}_J)$ is bounded by the sum of entries in the fourth row of Pascal's triangle, which is 16. Therefore, we establish the desired bounds for the eigenvalues. \square

References

- Agapiou, S. and Castillo, I. (2023). Heavy-tailed Bayesian nonparametric adaptation. *arXiv preprint arXiv:2308.04916*.
- Bach, P. and Klein, N. (2021). Posterior concentration rates for Bayesian penalized splines. *arXiv preprint arXiv:2109.04288*.
- Baladandayuthapani, V., Mallick, B. K., and Carroll, R. J. (2005). Spatially adaptive Bayesian penalized regression splines (P-splines). *Journal of Computational and Graphical Statistics*, 14(2):378–394.
- Bayarri, M. J., Berger, J. O., Forte, A., and García-Donato, G. (2012). Criteria for Bayesian model choice with application to variable selection. *The Annals of Statistics*, 40(3):1550–1577.
- Belitser, E. and Serra, P. (2014). Adaptive priors based on splines with random knots. *Bayesian Analysis*, 9(4):859–882.
- Brezger, A. and Lang, S. (2006). Generalized structured additive regression based on Bayesian P-splines. *Computational Statistics & Data Analysis*, 50(4):967–991.
- Cole, T. J. and Green, P. J. (1992). Smoothing reference centile curves: the LMS method and penalized likelihood. *Statistics in Medicine*, 11(10):1305–1319.
- De Boor, C. (1978). *A Practical Guide to Splines*, volume 27. springer-verlag New York.
- De Jonge, R. and Van Zanten, J. (2012). Adaptive estimation of multivariate functions using conditionally Gaussian tensor-product spline priors. *Electronic Journal of Statistics*, 6:1984–2001.
- Denison, D., Mallick, B., and Smith, A. (1998). Automatic Bayesian curve fitting. *Journal of the Royal Statistical Society: Series B (Statistical Methodology)*, 60(2):333–350.
- DiMatteo, I., Genovese, C. R., and Kass, R. E. (2001). Bayesian curve-fitting with free-knot splines. *Biometrika*, 88(4):1055–1071.
- Eilers, P. H. and Marx, B. D. (1996). Flexible smoothing with B-splines and penalties. *Statistical Science*, 11(2):89–121.
- Fahrmeir, L. and Kneib, T. (2009). Propriety of posteriors in structured additive regression models: Theory and empirical evidence. *Journal of Statistical Planning and Inference*, 139(3):843–859.
- George, E. and Foster, D. P. (2000). Calibration and empirical Bayes variable selection. *Biometrika*, 87(4):731–747.
- Ghosal, S., Ghosh, J. K., and van Der Vaart, A. W. (2000). Convergence rates of posterior distributions. *The Annals of Statistics*, 28(2):500–531.

- Ghosal, S. and van der Vaart, A. (2007). Convergence rates of posterior distributions for noniid observations. *The Annals of Statistics*, 35(1):192–223.
- Ghosal, S. and van der Vaart, A. (2017). *Fundamentals of Nonparametric Bayesian Inference*, volume 44. Cambridge University Press.
- Gray, R. M. et al. (2006). Toeplitz and circulant matrices: A review. *Foundations and Trends® in Communications and Information Theory*, 2(3):155–239.
- Hennerfeind, A., Brezger, A., and Fahrmeir, L. (2006). Geoadditive survival models. *Journal of the American Statistical Association*, 101:1065–1075.
- Hoeting, J. A., Madigan, D., Raftery, A. E., and Volinsky, C. T. (1999). Bayesian model averaging: a tutorial (with comments by M. Clyde, David Draper and EI George, and a rejoinder by the authors. *Statistical Science*, 14(4):382–417.
- Jeong, S. and Ghosal, S. (2021). Unified Bayesian theory of sparse linear regression with nuisance parameters. *Electronic Journal of Statistics*, 15(1):3040–3111.
- Jeong, S., Park, T., and van Dyk, D. A. (2022). Bayesian model selection in additive partial linear models via locally adaptive splines. *Journal of Computational and Graphical Statistics*, 31(2):324–336.
- Kang, G. and Jeong, S. (2023). Model selection-based estimation for generalized additive models using mixtures of g-priors: Towards systematization. *arXiv preprint arXiv:2301.10468*.
- Kass, R. E. and Raftery, A. E. (1995). Bayes factors. *Journal of the American Statistical Association*, 90(430):773–795.
- Kohn, R., Smith, M., and Chan, D. (2001). Nonparametric regression using linear combinations of basis functions. *Statistics and Computing*, 11:313–322.
- Lang, S. and Brezger, A. (2004). Bayesian P-splines. *Journal of Computational and Graphical Statistics*, 13(1):183–212.
- Laurent, B. and Massart, P. (2000). Adaptive estimation of a quadratic functional by model selection. *The Annals of Statistics*, 28(5):1302–1338.
- Li, Y. and Clyde, M. A. (2018). Mixtures of g-priors in generalized linear models. *Journal of the American Statistical Association*, 113(524):1828–1845.
- Liang, F., Paulo, R., Molina, G., Clyde, M. A., and Berger, J. O. (2008). Mixtures of g priors for Bayesian variable selection. *Journal of the American Statistical Association*, 103(481):410–423.
- Maruyama, Y. and George, E. I. (2011). Fully Bayes factors with a generalized g-prior. *The Annals of Statistics*, 39(5):2740–2765.
- Moreno, E., Bertolino, F., and Racugno, W. (1998). An intrinsic limiting procedure for model selection and hypotheses testing. *Journal of the American Statistical Association*, 93(444):1451–1460.

- Neal, R. M. (2003). Slice sampling. *The Annals of Statistics*, 31(3):705–767.
- Ning, B., Jeong, S., and Ghosal, S. (2020). Bayesian linear regression for multivariate responses under group sparsity. *Bernoulli*, 26(3):2353–2382.
- Ruppert, D. (2002). Selecting the number of knots for penalized splines. *Journal of Computational and Graphical statistics*, 11(4):735–757.
- Shen, W. and Ghosal, S. (2015). Adaptive Bayesian procedures using random series priors. *Scandinavian Journal of Statistics*, 42(4):1194–1213.
- Shen, X., Wolfe, D., and Zhou, S. (1998). Local asymptotics for regression splines and confidence regions. *The Annals of Statistics*, 26(5):1760–1782.
- Simpson, D., Rue, H., Riebler, A., Martins, T. G., and Sørbye, S. H. (2017). Penalising model component complexity: A principled, practical approach to constructing priors. *Statistical Science*, 32(1):1–28.
- Smith, M. and Kohn, R. (1996). Nonparametric regression using Bayesian variable selection. *Journal of Econometrics*, 75(2):317–343.
- Stone, C. J. (1982). Optimal global rates of convergence for nonparametric regression. *The Annals of Statistics*, 10(4):1040–1053.
- Ventrucci, M. and Rue, H. (2016). Penalized complexity priors for degrees of freedom in Bayesian P-splines. *Statistical Modelling*, 16(6):429–453.
- Wahba, G. (1977). Practical approximate solutions to linear operator equations when the data are noisy. *SIAM Journal on Numerical Analysis*, 14(4):651–667.
- Wainwright, M. J. (2019). *High-Dimensional Statistics: A Non-Asymptotic Viewpoint*, volume 48. Cambridge University Press.
- Wood, S. N. (2006). On confidence intervals for generalized additive models based on penalized regression splines. *Australian & New Zealand Journal of Statistics*, 48(4):445–464.
- Wood, S. N. (2011). Fast stable restricted maximum likelihood and marginal likelihood estimation of semiparametric generalized linear models. *Journal of the Royal Statistical Society Series B: Statistical Methodology*, 73(1):3–36.
- Wood, S. N. (2017). *Generalized Additive Models: an Introduction with R*. CRC press.
- Xiao, L. (2019). Asymptotic theory of penalized splines. *Electronic Journal of Statistics*, 13:747–794.
- Xue, L. (2009). Consistent variable selection in additive models. *Statistica Sinica*, 19:1281–1296.
- Yoo, W. W. and Ghosal, S. (2016). Supremum norm posterior contraction and credible sets for nonparametric multivariate regression. *The Annals of Statistics*, 44(3):1069–1102.

Zellner, A. (1986). On assessing prior distributions and bayesian regression analysis with g-prior distributions. *Bayesian Inference and Decision Techniques: Essays in Honor of Bruno de Finetti*, pages 233–243.

Zellner, A. and Siow, A. (1980). Posterior odds ratios for selected regression hypotheses. *Trabajos de Estadística e Investigación Operativa*, 31:585–603.